

Timing relationships and resulting communications challenges in relativistic travel[★]

David Messerschmitt^a, Ian Morrison^{b,c}, Thomas Mozdzen^d, Philip Lubin^e

^a*University of California at Berkeley, Department of Electrical Engineering and Computer Sciences, USA*

^b*Curtin University, International Centre for Radio Astronomy Research, Australia*

^c*Astro Signal Pty Ltd, Perth, Australia*

^d*Arizona State University, Department of Physics, USA*

^e*University of California at Santa Barbara, Department of Physics, USA*

Abstract

Communications between a spacecraft undertaking interstellar travel at near light speed to and from its launch site (the origin) and a landing site (the destination), as well as with other spacecraft, faces significant challenges. Photon-based communication is significantly impacted by classical effects, including large photon propagation delay, and relativistic effects, including time dilation experienced by clocks moving at high relative speeds. The timing of communications by photon transfer, as measured specifically by local clocks at origin and destination and aboard spacecraft, is analyzed and illustrated for concrete mission scenarios. These include a spacecraft experiencing indefinite constant self-acceleration, and a launch-landing mission, in which a spacecraft experiences constant acceleration for the first half of its cruise phase and a like deceleration for the second half. The origin and destination are assumed to be at rest within a common inertial frame with a wide range of fixed distances separating them. Several typical communication modes are considered, including one-way messaging, two-way message query with an expected response, and the one-way streaming of long program material such as a podcast or video. The local-clock relative timing experienced by the communicating entities including clock images (relation of transmit and receive clocks in one-way communication), the query-response latency (the elapsed time between a query message and reception of a message in response), and the time warping of a streaming program (nonlinear stretching or shrinking of the time axis) are included. In particular, large query-response latency, except for a short interval following launch or before landing, is a severe limit on remote control and social interaction. When photons must travel in the same direction as the spacecraft, communication blackouts strongly limit the periods of time during which communication is possible, and restrict the opportunities for both one-way and two-way communication.

Keywords: interstellar communications spacecraft relativistic

1. Introduction

Consider a spacecraft cruising between two at-rest locations (an origin and a destination) separated by large interstellar distances. Maintaining communications with the origin, destination, or with other spacecraft brings many benefits, from practical mission engineering and management, to scientific data, and to the psychological benefits of astronauts remaining in touch with the civilization left behind. However, interstellar travel with human astronauts necessitates high spacecraft velocities approaching the speed of light. Relativistic effects thereby come into play, and these can have extreme (and sometimes surprising) impacts on communications systems and capabilities.

In particular, a central result of relativity is that clocks in relative motion run at different relative rates. This means that a relativistic traveler's measurements of time are inconsistent with that of observers at the origin or destination. In isolation everyone is content with their own sense of time, but this affects the traveler's sense of connection to their environment. This includes affecting communication among travelers in motion with relativistic relative velocities, where clock inconsistency is directly apparent. In particular, it strongly affects perceptions of relative timing, which has to be taken into account in both the formulation and interpretation of communicated messages. This concept is explored analytically and quantitatively in this paper and applied to two simple mission profiles. See §Appendix A for a compilation of variables employed in the following.

2. Travelers' clocks in relativistic travel

Participants in interstellar travel, such as spacecraft (including instrumentation and possibly astronauts) and civilizations that launch such spacecraft, perceive time in terms of clocks that they carry along with other payloads and supplies. Suppose for one such participant \mathcal{A} the time measured by a clock that it carries is τ_a . This is called the *proper time* associated with \mathcal{A} , meaning “the time observed by a clock at rest relative to participant \mathcal{A} ”. Following [1] a more descriptive term for τ_a is \mathcal{A} 's *traveler's time*.

2.1. Clock images

For many purposes there is no concern about other participants' traveler's times. However any activity that involves two or more such participants, such as navigation or communication of information among them, emphasizes a relationship among their traveler's times.

Consider two spatially separated travelers in a one-dimensional space with spatial dimension x . These travelers are denoted by \mathcal{A} and \mathcal{B} , they have possibly distinctive velocities and accelerations as measured relative to x .

These travelers each carry their own clocks with them, and these clocks measure traveler's times τ_a and τ_b . In a communication context (the primary concern here) this relationship between \mathcal{A} and \mathcal{B} is created by *photon exchange*, in which \mathcal{A} emits a photon at its traveler's time τ_a and that photon is detected by \mathcal{B} at its traveler's time τ_b . Thus \mathcal{A} is in control, since this traveler chooses τ_a , and τ_b is determined by the position of \mathcal{A} at the instant of photon emission as well as the time-dependent position of \mathcal{B} (and the related measurement of its local clock) during the photon's propagation through spacetime.

Define two related functions $\Psi_{\mathcal{A}\Rightarrow\mathcal{B}}$ and $\Omega_{\mathcal{A}\Rightarrow\mathcal{B}}$ that establish a causal relationship between these times as

$$\tau_b = \Psi_{\mathcal{A}\Rightarrow\mathcal{B}}[\tau_a] \text{ and } \tau_a = \Psi_{\mathcal{A}\Rightarrow\mathcal{B}}^{-1}[\tau_b] = \Omega_{\mathcal{A}\Rightarrow\mathcal{B}}[\tau_b]. \quad (1)$$

The interpretation of $\Psi_{\mathcal{A}\Rightarrow\mathcal{B}}$ is the time τ_b at which \mathcal{B} detects a photon that was emitted by \mathcal{A} at time τ_a , assuming that this photon propagates from \mathcal{A} to \mathcal{B} , assumed to be at the vacuum speed of light c . The inverse $\Omega_{\mathcal{A}\Rightarrow\mathcal{B}}$ always exists because on physical grounds $\Psi_{\mathcal{A}\Rightarrow\mathcal{B}}$ is a strictly monotonically increasing function. The domain and codomain (range) of $\Psi_{\mathcal{A}\Rightarrow\mathcal{B}}$ is a subset of the real numbers. The domain of $\Omega_{\mathcal{A}\Rightarrow\mathcal{B}}$ is the range of $\Psi_{\mathcal{A}\Rightarrow\mathcal{B}}$ and vice versa.

The relationship $\Psi_{\mathcal{A}\Rightarrow\mathcal{B}}$ is determined by kinematic variables (relative positions, velocities, and accelerations of \mathcal{A} and \mathcal{B}). Similarly the inverse function $\Omega_{\mathcal{A}\Rightarrow\mathcal{B}} = \Psi_{\mathcal{A}\Rightarrow\mathcal{B}}^{-1}$ infers, under the same conditions, the time of emission τ_a corresponding to an observed detection time τ_b . Function $\Psi_{\mathcal{A}\Rightarrow\mathcal{B}}$ is called the *clock image* [1] because of its analogy to a picture or image of \mathcal{A} taken by \mathcal{B} .

Example: If \mathcal{A} wants to send \mathcal{B} a “happy birthday” greeting, the relevant birthday is defined in accordance with τ_b . If \mathcal{A} wants that greeting (sent as a message carried by photons) to arrive at $\tau_b = \tau_r$, corresponding to say 8:00am on \mathcal{B} 's next birthday, then \mathcal{A} should originate that message at its own traveler's time $\tau_a = \Omega_{\mathcal{A}\Rightarrow\mathcal{B}}[\tau_r]$.

2.2. Reversing direction of propagation

The direction of the arrow in the designation $\mathcal{A}\Rightarrow\mathcal{B}$ specifies the direction of photon transfer from \mathcal{A} to \mathcal{B} and hence establishes a cause-and-effect relationship between the emission and detection of a photon and the resulting timing relationship. The alternative $\mathcal{B}\Rightarrow\mathcal{A}$ implies a transfer from \mathcal{B} to \mathcal{A} and is markedly different due to a reversal of the direction of propagation for a photon relative to the motion of \mathcal{A} and \mathcal{B} . Thus $\Psi_{\mathcal{B}\Rightarrow\mathcal{A}}$ cannot be inferred from $\Psi_{\mathcal{A}\Rightarrow\mathcal{B}}$ in any straightforward way; that is, $\Psi_{\mathcal{A}\Rightarrow\mathcal{B}}$ and $\Psi_{\mathcal{B}\Rightarrow\mathcal{A}}$ must be determined independently.

Example: Continuing the last example, \mathcal{B} receiving a birthday greeting message at $\tau_b = \tau_r$ can infer that the message was sent at \mathcal{A} 's traveler's time

$\tau_a = \Omega_{\mathcal{A} \Rightarrow \mathcal{B}}[\tau_r]$. Further if \mathcal{B} immediately replies to that message at $\tau_b = \tau_r$, then the time that message will arrive at \mathcal{A} , according to \mathcal{A} 's local clock, can be inferred by \mathcal{B} to be $\tau_a = \Psi_{\mathcal{B} \Rightarrow \mathcal{A}}[\tau_r]$ (note the switch from $\Omega_{\mathcal{A} \Rightarrow \mathcal{B}}$ to $\Psi_{\mathcal{B} \Rightarrow \mathcal{A}}$). Traveler \mathcal{B} may want to take this arrival time into account in any return message, such as relating it to \mathcal{A} 's own age at the traveler's time τ_a at which \mathcal{A} receives the message.

2.3. Compact notation for clock image compositions

In the following it will often be the case that a given scenario of interest involves two or more photon exchanges. Anticipating that need, we employ a standard notation for the composition of functions.

2.3.1. Communication among three travelers

This is illustrated by a configuration in which there are three travelers $\{\mathcal{A}, \mathcal{B}, \mathcal{C}\}$ along the spatial axis x in this order. If \mathcal{A} emits a photon at time τ_a in the $+x$ direction, which is detected by \mathcal{B} at time τ_b , suppose that \mathcal{B} in response to that detection immediately emits a photon which is in turn detected by \mathcal{C} at time τ_c . In that case the relationship among $\{\tau_a, \tau_b, \tau_c\}$ is summarized by

$$\tau_b = \Psi_{\mathcal{A} \Rightarrow \mathcal{B}}[\tau_a] \quad (2)$$

$$\tau_c = \Psi_{\mathcal{B} \Rightarrow \mathcal{C}}[\tau_b] \quad (3)$$

$$\implies \tau_c = \Psi_{\mathcal{B} \Rightarrow \mathcal{C}}[\Psi_{\mathcal{A} \Rightarrow \mathcal{B}}[\tau_a]]. \quad (4)$$

In the following, we denote the composition of two clock images by the equivalent but arguably more transparent representation

$$\tau_c = (\Psi_{\mathcal{B} \Rightarrow \mathcal{C}} \circ \Psi_{\mathcal{A} \Rightarrow \mathcal{B}})[\tau_a]. \quad (5)$$

With the composition operator “ \circ ”, the invocation of the functions is from right to left. Note that there is an assumption of immediacy; namely, \mathcal{B} responds to its own detection of a photon by immediately emitting a new photon. In addition, the domain and range of the clock image functions has to be considered, since it is possible to establish nonsensical conditions that violate these constraints.

Example: \mathcal{A} wants to wish \mathcal{B} a happy birthday, with the message arriving at \mathcal{B} 's traveler's time $\tau_b = \tau_r$ appropriate for the birthday. As in the earlier example, \mathcal{A} should originate that message at time $\tau_a = \Omega_{\mathcal{A} \Rightarrow \mathcal{B}}[\tau_r]$. Now suppose \mathcal{A} wishes to remind a third traveler \mathcal{C} that it is \mathcal{B} 's birthday by sending to \mathcal{C} a message “Please immediately send a birthday greeting to \mathcal{B} , and if you do so it will arrive at the appropriate time”. To satisfy that promise, \mathcal{C} should receive \mathcal{A} 's message at $\tau_c = \Omega_{\mathcal{C} \Rightarrow \mathcal{B}}[\tau_r]$. Thus \mathcal{A} should originate that reminder message to \mathcal{C} at its own traveler's time

$$\tau_a = \Omega_{\mathcal{A} \Rightarrow \mathcal{C}}[\tau_c] = \Omega_{\mathcal{A} \Rightarrow \mathcal{C}}[\Omega_{\mathcal{C} \Rightarrow \mathcal{B}}[\tau_r]] = (\Omega_{\mathcal{A} \Rightarrow \mathcal{C}} \circ \Omega_{\mathcal{C} \Rightarrow \mathcal{B}})[\tau_r]. \quad (6)$$

This requirement becomes nonsensical if either τ_r falls outside the domain of function $\Omega_{C \Rightarrow B}$, or if $\tau_c = \Omega_{C \Rightarrow B}[\tau_r]$ falls outside the domain of function $\Omega_{A \Rightarrow C}$. This will occur whenever $\{\mathcal{A}, \mathcal{B}, \mathcal{C}\}$ are too distant and the traveler's clocks are such that it is impossible to get one or more messages to the appointed destinations by the appointed time.

The “o” version in Eq.(6) is quicker and easier to interpret, and with a bit of practice also becomes straightforward to specify directly.

2.3.2. Query-response communication

Another common situation is *query-response* communication between two travelers. Suppose that \mathcal{A} wishes to receive a response from \mathcal{B} to its own query. This involves two one-way communications, first $\mathcal{A} \Rightarrow \mathcal{B}$ conveying the query followed by $\mathcal{B} \Rightarrow \mathcal{A}$ conveying the response back to \mathcal{A} . Suppose the original query traveler's time is at traveler's time τ_{a1} , \mathcal{B} responds immediately, and the response arrives back at \mathcal{A} at traveler's time τ_{a2} . Then we can infer that $\tau_{a2} = (\Psi_{\mathcal{B} \Rightarrow \mathcal{A}} \circ \Psi_{\mathcal{A} \Rightarrow \mathcal{B}})[\tau_{a1}]$. Note that the direction of photon travel is reversed in the two invocations of clock image Ψ .

Typically \mathcal{A} will be interested in the elapsed time $(\tau_{a2} - \tau_{a1})$ (as measured by its local clock) between the time it initiates a query and the time that it receives a response. This suggests a new function called the *query-response latency*, which is denoted by $\mathfrak{L}_{\mathcal{A} \Leftrightarrow \mathcal{B}}[\tau]$,

$$\begin{aligned} \mathfrak{L}_{\mathcal{A} \Leftrightarrow \mathcal{B}}[\tau_{a1}] &= (\Psi_{\mathcal{B} \Rightarrow \mathcal{A}} \circ \Psi_{\mathcal{A} \Rightarrow \mathcal{B}})[\tau_{a1}] - \tau_{a1} \\ &= (\Psi_{\mathcal{B} \Rightarrow \mathcal{A}} \circ \Psi_{\mathcal{A} \Rightarrow \mathcal{B}} - \mathbb{1})[\tau_{a1}] \end{aligned} \quad (7)$$

where $\mathbb{1}$ is the identify function. This latency depends on the traveler's time τ_{a1} corresponding to the initiating query. The notation $\mathcal{A} \Leftrightarrow \mathcal{B}$ denotes a bi-directional communication between \mathcal{A} and \mathcal{B} that is initiated by \mathcal{A} .

Example: If \mathcal{A} 's query is “how do I repair or circumvent my broken CO₂ scrubber” then circumstances favor a quick (low latency) response!

There is an implicit traveler's time $\tau_b = \Psi_{\mathcal{A} \Rightarrow \mathcal{B}}[\tau_{a1}]$ at which \mathcal{B} receives the query and is expected to immediately generate a response. This value of τ_b will often influence \mathcal{B} 's response.

Example: If \mathcal{A} 's query is “what time do you have”, the response would be something like “my current time is $\tau_b = 1.645$ yr following my launch”. From that response, if \mathcal{A} is knowledgeable of the navigation plan for \mathcal{B} then trajectory coordinates $\{x_b, t_b\}$ of \mathcal{B} at the instant of response could also be inferred (see §5.1).

2.4. Factors determining clock images

There are three factors that collectively influence and determine the clock image $\Psi_{\mathcal{A}\Rightarrow\mathcal{B}}$ in the context of communication by photon exchange:

Propagation delay. In photon exchange there is a light-speed propagation delay between emission and detection. If \mathcal{A} is the photon emitter, the delay depends on \mathcal{A} 's position at the time of emission, but not on \mathcal{A} 's subsequent motion. The delay then depends on \mathcal{B} 's motion throughout the photon propagation, since that motion affects \mathcal{B} 's distance at the subsequent photon detection.

Relativistic time dilation. In the event of any relative motion, τ_a and τ_b advance at inconsistent rates.

Clock initialization. Should the clocks τ_a and τ_b have arbitrary initializations, this would result in an unknown or unspecified mutual offset. To eliminate this ambiguity we assume that the clocks are *synchronized* in a sense that depends on the mission context (see §4.3).

3. Spacecraft trajectories

In order to infer the clock image functions, it is necessary to know the *trajectory* of the two travelers exchanging photons. In the case of a spacecraft traveler, its *mission* describes this trajectory in the context of a concrete objective (such as scientific investigation or exploration). The clock image $\Psi_{\mathcal{A}\Rightarrow\mathcal{B}}$ and query-response latency $\mathfrak{L}_{\mathcal{A}\Leftrightarrow\mathcal{B}}$ are powerful tools in understanding the limits to communication in the context of an interstellar mission, one that has the objective of reaching the vicinity of stars other than our Sun.

Communication challenges are best illustrated in the context of concrete interstellar mission examples. The goal here is to emphasize communications to and from a spacecraft traveling at relativistic speed (a significant fraction of the speed of light), while avoiding complications wrought by complex mission scenarios. Therefore two simple (and yet recognizably idealized) trajectories and associated missions are considered in the following:

Indefinite acceleration. Following launch from some stationary origin, the spacecraft and its payload experience a constant acceleration that continues indefinitely. In this case “acceleration” is that measured by an accelerometer carried by the spacecraft.

Canonical mission. The spacecraft is launched from a stationary origin and subsequently lands on a stationary destination. To this end it experiences a constant acceleration for half the distance from origin to destination,

followed by a constant deceleration (with the same magnitude) for the remaining distance.

The assumptions and details of these two trajectories are now considered further.

3.1. *Indefinite acceleration assumptions*

The *self-acceleration* (sometimes called *proper acceleration*) of a spacecraft is that measured by an accelerometer carried by the spacecraft. Significantly this is the acceleration imparted by the propulsion subsystem, and as well is the acceleration experienced by the payload, including possibly a human crew.

Indefinite acceleration makes the assumption of a constant self-acceleration with a numerical value α starting at the instant of launch (from a state of rest) and continuing thereafter, with no defined ending time. Of course maintaining acceleration indefinitely is not physically realizable (since it would require infinite energy expenditure) but this assumption results in a simple and analytically tractable *hyperbolic* trajectory (see §6). Further, a canonical mission trajectory is readily inferred based on a limited-time initial segment of a hyperbolic trajectory combined with the symmetry of the acceleration profile (see §7).

3.2. *Canonical mission architecture*

A typical interstellar mission has the objective of landing on some alien body, and is also physically realizable since its total energy expenditure is finite. In such a mission, a spacecraft is presumed to be launched from one stationary body, the *origin*, and to subsequently land on another stationary body, its *destination*. Typical origins and destinations are planets (for example Earth or Moon for an origin and an exoplanet for a destination).

The *canonical* mission is the simplest mission with this objective, and is illustrated in Fig.1. A spacecraft is propelled during a *cruise* phase with a constant self-acceleration for the first half of the journey and a constant (equal-in-magnitude) deceleration for the second half of the journey,

Although the origin and destination will generally be in relative motion, their relative velocity will generally be insignificant compared to the speed of light. Thus in our canonical mission scenario any relative motion between origin and destination is neglected and they are assumed to be inertial (not accelerating) relative to a common inertial frame S .

Our primary concern here is communication between the spacecraft and either origin or destination during the cruise phase. Although such a mission is presently beyond human technological capabilities and available energy resources, it is still worthwhile and interesting to consider (as we do here) the implications of timing relationships among these entities during the mission. The physical

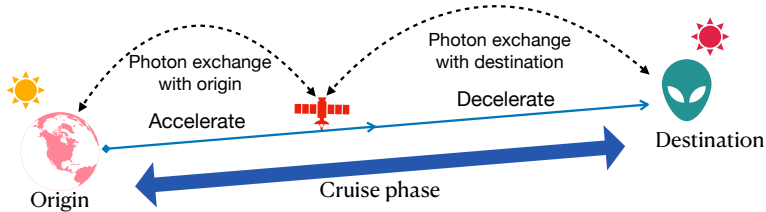


Figure 1: Illustration of the cruise phase of a canonical mission for a self-propelled spacecraft. At rest at the origin, beginning with launch it experiences constant self-acceleration for the first half of the distance to the destination followed by a constant self-deceleration (with the same magnitude) for the second half, at rest at the instant of landing on the destination. The origin and destination are themselves assumed to be indefinitely at rest relative to a common inertial frame S .

obstacles to communications uncovered is one among many important considerations in determining whether the large investments required to enable and execute interstellar travel are justified.

In the case of a mission carrying human astronauts, those astronauts (as well as any biological material they carry, such as plants, animals, or food) have to survive the accelerations endemic to the journey. While equipment can be designed to withstand large accelerations or weightlessness, biological material originating from a planetary environment is vulnerable to conditions not endemic to that environment, including large accelerations and weightlessness. To address this, in numerical examples we assume a so-called 1- g mission, which chooses a constant acceleration magnitude equal to Earth gravity, or $\alpha = \pm g$, thereby creating a spacecraft environment that replicates the Earth’s surface in this respect.

4. Relativistic effects on spacecraft trajectories

When traveling near the speed of light c , relativistic effects strongly affect the relationship between the spacecraft and its environment.

4.1. Travelers’ clocks

Following the description in §2, the canonical mission involves three travelers of interest: the origin \mathcal{O} , the spacecraft \mathcal{C} , and the destination \mathcal{D} . (Although \mathcal{O} and \mathcal{D} are assumed to be inertial, they can still be considered “travelers” in a degenerate sense.) The three travelers carry clocks measuring, respectively, traveler’s times $\tau_{\mathcal{O}}$, $\tau_{\mathcal{C}}$, and $\tau_{\mathcal{D}}$. (If this is not physically true of \mathcal{D} because it is technology-sterile, this remains useful for analytical purposes).

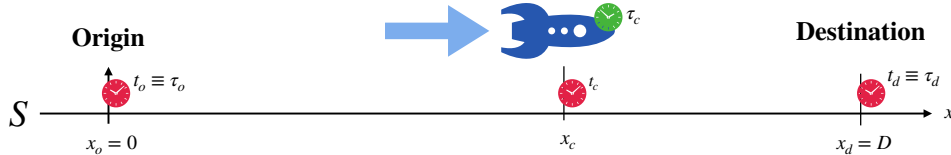


Figure 2: Illustration of the coordinates of a spacecraft's trajectory as a function of distance x and coordinate time t with respect to inertial frame S . The spatial coordinate x of the origin, spacecraft, and destination are labeled $\{x_o = 0, x_c, x_d = D\}$. Clocks which measure coordinate times t at those positions measure times labeled $\{t_o, t_c, t_d\}$. While t_o will likely be measured by a physical clock, $\{t_c, t_d\}$ may be notional (rather than physical) clocks. In addition there are three traveler's (proper) times $\{\tau_o, \tau_c, \tau_d\}$ carried by the respective travelers. The coordinate and traveler's clocks can be considered to be one and the same at the origin and destination, but differ for the spacecraft position x_c due to their relative motion.

4.2. Inertial frame and coordinate times

The location of the clocks of interest and a notation for their respective times are illustrated in Fig.2. The inertial frame S defined previously can be presumed to have 1-D spatial dimension x , as well as coordinate time t defined as the time measured by any clock at rest with respect to S . The speed of light as measured by $\{x, t\}$ is a constant c , and this allows for the determination of propagation delays. In the case of \mathcal{O} and \mathcal{D} their traveler's clocks are also at rest with respect to S , and thus they can be considered to have coordinate times $t_o \equiv \tau_o$ and $t_c \equiv \tau_c$. The coordinate time t_x at an arbitrary intermediate position $0 < x < D$ is defined as the time that would be measured by a clock at rest at that location, and generally $\tau_c \neq t_c$ due to the relative motion of the respective clocks. All clocks of interest can have a fixed offset dependent on their initialization. Taken together, the location of a traveler is quantified by its three coordinates $\{\tau, x, t\}$.

4.3. Clock synchronization

While $\{t_o, t_c, t_d\}$ run at identical rates (since they possess no relative motion), there remains the question of their appropriate initialization, and likewise the initialization of traveler's times $\{\tau_o, \tau_c, \tau_d\}$. The presumption of $\tau_o \equiv t_o$ and $\tau_d \equiv t_d$ defines the synchronization of two of the six clocks of interest. It is natural to assume that $t_o = \tau_o = \tau_c = 0$ at the instant of launch, since the respective clocks are co-located and thus can be simultaneously initialized.

The remaining two times $\{t_c, t_d\}$ are not measured by clocks co-located with one another or with t_o , and thus their initialization is more challenging. We assume that both are *synchronized* with t_o , meaning that a measurement of the light-speed c using $\{t_o, t_c, t_d\}$ yields the correct value c . This synchronization is also suitable for characterizing clock images. That is, a photon emitted at time $t_o = 0$ at the origin is detected at time $t_d = x_c/c$ at x_c and at $t_d = D/c$ at the destination.

Example: If \mathcal{O} sends a message to \mathcal{D} as it initializes its local clock to $t_o = 0$, that message traveling at the speed of light can upon arrival trigger an initialization of the destination clock to $t_d = D/c$, assuming that \mathcal{D} has knowledge of message propagation distance D .

When the propagation distance is unknown to the travelers, clock synchronization requires bi-directional photon exchange protocols [1].

4.4. Measures of mission elapsed time

The *mission-elapsed time* (MET) is the cumulative time elapsed for the spacecraft to reach some position x_c during the spacecraft cruise phase. There are two versions, depending on what clock is used to measure that elapsed time. The mission elapsed coordinate time (MECT) is measured by coordinate time t_c , whereas the mission-elapsed traveler's time (METT) is measured by the spacecraft's traveler's time τ_c , where we follow the convention that $\tau_c=0$ at the instant of launch.

The spacecraft speed must be less than light-speed c relative to S , and thus $\text{MECT} > x_c/c$. Due to relativistic time dilation, the spacecraft's traveler's clock runs more slowly than its respective coordinate clock, and thus $\text{METT} \ll \text{MECT}$ (see §6.2) Thus it is entirely possible that $\text{METT} \ll x_c/c$, so that, as measured by the traveler's clock, the light-speed limit has been exceeded.

An alternative trajectory could include a ballistic (constant speed) phase in its center. In this case the ballistic phase would be bracketed by equal durations of acceleration and deceleration. Our canonical mission includes no such ballistic phase. This alternative would have minimal impact on the MECT at the time of landing, because with or without the ballistic phase the spacecraft speed is very near to c for most of the cruise. However, as will be seen, omitting the ballistic phase beneficially and substantially reduces METT (to the benefit of resources consumed on the spacecraft and biological aging).

5. Communication with a spacecraft

Especially for a spacecraft with human astronauts, persistent communication during the entire mission would be desirable during the cruise phase, as opposed to following landing only. However, except for relatively brief time periods shortly after launch and before landing, the spacecraft will be traveling at nearly the speed of light. This presents special issues as we will see. Post-landing the spacecraft is assumed to be at rest in S , so the situation is far simpler.

During the cruise phase there are four instances of communication represented by $\mathcal{O} \Rightarrow \mathcal{C}$, $\mathcal{C} \Rightarrow \mathcal{O}$, $\mathcal{C} \Rightarrow \mathcal{D}$, and $\mathcal{D} \Rightarrow \mathcal{C}$. For each of these cases the clock image Ψ and its inverse Ω characterize the timing of the communication as affected by both propagation delay and relativistic time dilation (see §2.1).

The query-response latency $\mathfrak{L}_{\mathcal{A} \leftrightarrow \mathcal{B}}$ characterizes the delay experienced by a traveler in a two-way communication. Instances of these involving the spacecraft include $\mathcal{O} \leftrightarrow \mathcal{C}$, $\mathcal{C} \leftrightarrow \mathcal{O}$, $\mathcal{C} \leftrightarrow \mathcal{D}$, and $\mathcal{D} \leftrightarrow \mathcal{C}$. This latency can be determined by the composition of one clock image Ψ for the query and another for the response. Since travelers may not be fully cognizant of one another's trajectories, both query and response messages are likely to include a time-stamp confirming or revealing the local traveler's time.

Here we summarize the results of this analysis absent mathematical justification, followed in §6 by an analysis employing the special theory of relativity (SR).

5.1. Spacecraft trajectory

The spacecraft trajectory reveals the evolution of its position x_c in S vs time, specifically $\{\tau_c, x_c, t_c\}$. This can be interpreted as space time $\{x_c, t_c\}$ relative to S coordinates as parameterized by the traveler's time τ_c . S provides a common reference for measuring photon propagation delays, time dilation effects for the spacecraft traveler's clock, and clock images.

In the case of a spacecraft, τ_c governs the operation of the spacecraft instrumentation and is very significant to any human astronauts (governing their heart rate, circadian rhythm, etc). On the other hand, t_c matters greatly to navigation systems aboard the spacecraft and at the origin (which measure and control spacecraft kinematics relative to an inertial frame S), to controllers and operators at the origin and destination, and determines photon propagation delay.

5.2. Event horizon

The simpler indefinite self-acceleration trajectory is illustrated in Fig.3. A convenient parameter describing this trajectory is the *event horizon* $t_H = c/\alpha$. The physical significance of t_H is the earliest coordinate time for which a photon leaving the origin never intersects the spacecraft trajectory, and hence will never be detected onboard the spacecraft.

Three photon trajectories (each linear with unity slope) are compared to the spacecraft in Fig.3. The first is a photon emitted from the origin at the instant of spacecraft launch. The spacecraft has to travel more slowly than this photon, since it cannot exceed lightspeed c , and thus its trajectory always falls above the photon's trajectory (its coordinate time to reach any position x_c has to be larger). As the spacecraft speed approaches light-speed c , its trajectory exponentially approaches (but never intersects) that of a photon emitted from the origin at $t_o = t_H$. The trajectory of any photon emitted from the origin for $t_o \geq t_H$, which falls inside the shaded region on Fig.3, never intersects the spacecraft trajectory, and hence no such photon can ever be detected by the spacecraft. A typical case is the photon emitted at $t_o = 2t_H$ as shown.

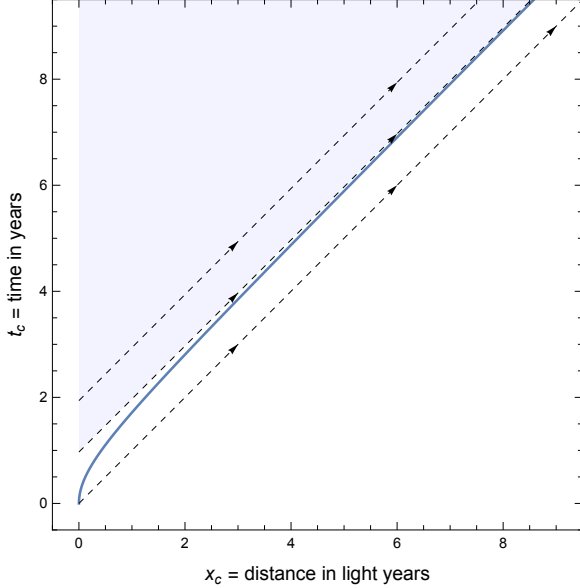


Figure 3: The trajectory of an indefinite 1-g self-acceleration spacecraft with $\alpha_c = +g$ and event horizon $t_H = 0.97$ yr is plotted over an elapsed traveler's time of $0 \leq \tau_c \leq 3$ yr. See §6.4 for a derivation of this trajectory. Also shown as dashed lines are the trajectories of a photon emission from the *origin* at three coordinate times $t_o \in \{0, t_H, 2t_H\}$ in the $+x$ direction. Each is a straight line with slope +1 on a plot with time units of years and distance units of light years.

In summary, photon emissions originating from the origin beyond the event horizon (shown as the shaded area) are invisible to spacecraft experiencing indefinite acceleration. The result is a communications *blackout* from the origin to the spacecraft. While such a blackout is not present for the canonical mission, the value of t_H has a significant impact on clock images in that case as well.

5.3. Spacecraft communication with origin and destination

The trajectory of a spacecraft on the canonical mission is illustrated in Fig.4 together with some typical trajectories for photons exchanged to and from the origin \mathcal{O} and destination \mathcal{D} . Due to the time-reversal symmetry of the acceleration/deceleration, the second half of the canonical mission trajectory is simply a mirror image of the first half (see §7).

The shaded regions in Fig.4 represent photons that intercept \mathcal{C} 's trajectory, and thus were either omitted or can be detected during \mathcal{C} 's cruise phase. These photons are deemed to be *productive*, in the sense that they can be employed as a basis for communication during \mathcal{C} 's cruise phase. Photon trajectories outside these shaded regions must be emitted or detected while \mathcal{C} is at rest at \mathcal{O} pre-launch or at \mathcal{D} post-landing. \mathcal{C} 's payload (including possibly human astronauts)

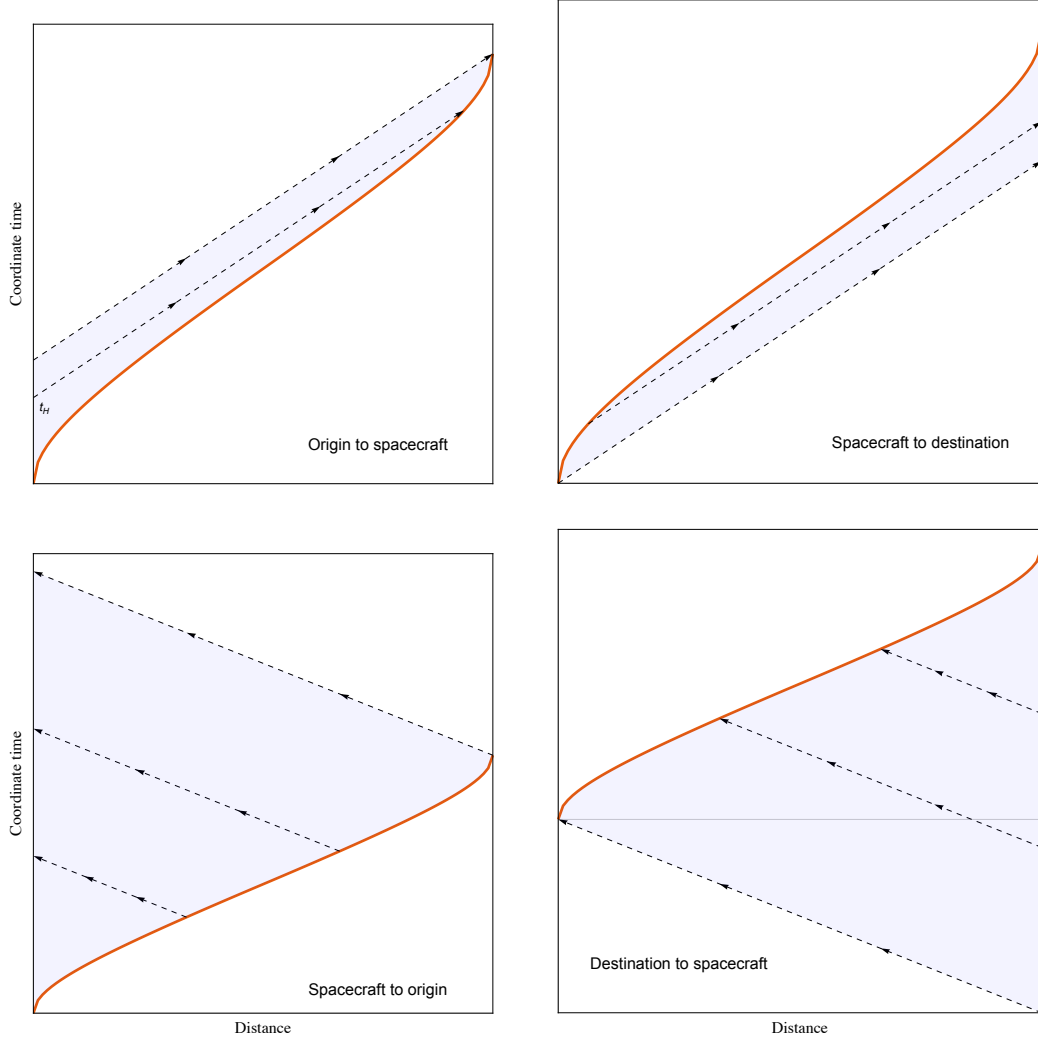


Figure 4: Illustration of the time constraints on communication during a spacecraft's travel from launch to landing for the canonical mission. The spacecraft trajectory is the solid line, and photon trajectories to and from the spacecraft and to and from the origin and destination are shown as dashed lines. Each shaded region represents the ensemble of all feasible photon trajectories which intersect the spacecraft trajectory during its cruise phase. The most significant influence on this ensemble shape is the direction of photon propagation.

is governed by a local clock measuring traveler's time τ_c (represented only by parameterization in Fig.4).

In the direction $O \Rightarrow C$, a photon emitted from the origin over the coordinate-time interval $0 < t_o < \sim 2t_H$ can be detected by the spacecraft during its cruise phase

(later-emitted photons reach the spacecraft following landing at the destination). The factor $\sim 2t_H$ is the composition of $\sim t_H$ for the first half and another $\sim t_H$ (due to the mirror-image symmetry) for the second half. (The precise range of times is slightly smaller than $\sim t_H$, since the positive self-acceleration of the spacecraft is terminated at the halfway point.)

A set of important distinctions and conclusions can be drawn from Fig.4:

- From the perspective of spacecraft C , detection of photons originating from both $\{O, D\}$ and emission of photons toward both $\{O, D\}$ are productive during the entirety of the cruise phase. This constitutes C 's entire cruise-phase METT.
- Consider the perspective of O and D and photons either emitted or detected that propagate in the same direction as C 's velocity (which is the direction O to D). That includes directions $O \Rightarrow C$ and $C \Rightarrow D$. These photons are productive during a relatively short coordinate-time duration $\sim 2t_H$ in both cases. Since $\text{MECT} = \sim (D/c + 2t_H)$ for the entirety of the cruise phase, there is a long coordinate-time duration $\sim D/c$ overlapping the METT over which no photon emissions and detections can be productive.
- Consider again the perspective of O and D , but in this case photons either emitted or detected propagate in the opposite direction to the spacecraft C 's velocity. This includes directions $C \Rightarrow O$ and $D \Rightarrow C$. Those photons are productive during a long coordinate-time duration which is about *double* the METT.
- There is a substantial distinction between the productive coordinate-time duration of communication in both directions as compared to the spacecraft's METT. This represents a *time-warping* effect, in which communication signals always appear to have distinctive time axes at transmitter and receiver (see §5.7). Time-warping is distinct from relativistic time-dilation (see §6.2), and is considerably more extreme in its effect. While time-warping is affected by time-dilation, it is primarily a manifestation of the observation that photons propagating in the same direction as the spacecraft have difficulty "catching up with" or "getting out ahead of" a spacecraft traveling at near the speed of light c .

The MECT at landing, from the perspective of the origin O or destination D , defines a coordinate-time period coinciding with the cruise phase of spacecraft C . Ideally communication to and from the spacecraft would be possible during the entirety of this MECT. Whenever such communication is not possible (resulting from non-productive photon emissions or detections), this constitutes a *communication blackout*, which is summarized in Tbl.1. The practical manifestation of

Table 1: Communication blackout conditions

$O \Rightarrow C$	Communications from O does not reach the spacecraft C during the cruise phase except for a coordinate-time duration $\sim 2t_H$ immediately following launch. Such communications do arrive following landing, while the spacecraft is at rest at the destination.
$C \Rightarrow O$ and $D \Rightarrow C$	Communication is possible during C 's entire cruise phase.
$C \Rightarrow D$	D receives no communication from C initiated during its cruise phase except for a coordinate-time duration $\sim 2t_H$ immediately preceding landing.

these blackouts is that C (or D) cannot be informed of any events at O (or C) except for a short period of coordinate-time duration $\sim 2t_H$ (about two years for a 1-g canonical mission) immediately following launch (or preceding landing).

5.4. Mission elapsed time at landing

The mission elapsed times can be considered and compared from a traveler's and coordinate time perspective. The traveler's perspective is simpler, since $METT \equiv \tau_c$ for cruising distance $0 < x \leq x_c$. There are three coordinate times $\{t_o, t_c, t_d\}$ that differ in their initialization, but $MECT \equiv t_c$ is the correct choice for the MECT when the spacecraft is at position x_c , since it defines the coordinate time at that position. The initializations of $\{t_o, t_c\}$ are set to correctly measure the speed of a photon, which implies that they also correctly measure a photon's propagation time $t_c - t_o$ from $x = 0$ to $x = x_c$. It follows that those initializations are also the correct measure of MECT for a spacecraft.

The MECT and METT at the time of landing are quite different. The landing-time MECT of the canonical 1-g mission is $MECT = \sim(D/c + 2t_H)$. This is an asymptote for large D , with the precise value plotted in Fig.5 ((see §5.3). The METT is plotted in Fig.6, and is much smaller ($METT \ll MECT$) due to relativistic time dilation.

This distinction between MECT and METT is very significant for spacecraft designers, since METT governs all time-dependent aging and resource utilization, including the time period over which self-acceleration has to be maintained, on-board energy, wear and tear of equipment, life support supplies for human astronauts including food and oxygen, and the biological aging of the astronauts. Even for a journey to the nearest galaxy Andromeda ($D \approx 2.5 \cdot 10^6$ ly) the total canonical-mission METT at landing falls within a typical human lifetime.

Another consideration is the timekeeping aspect of communications. This affects the perception of the communication from the receiving end, but the transmitting end should also be aware of any time limitations on their ability to convey information or events.

Example: Consider the uplink (direction $O \Rightarrow C$). A spacecraft crew that travels

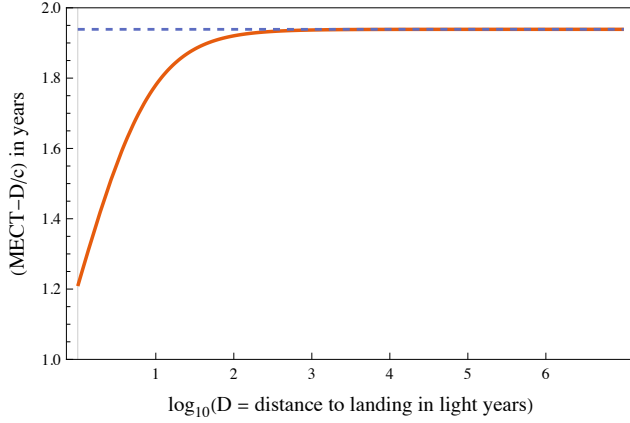


Figure 5: A plot of the excess of the MECT over the time for a photon to reach the destination for the canonical mission of Fig.1. This is compared to twice the event horizon ($2t_H$) as the dashed line. The horizontal axis is the log of distance $\log D$ for $1 \leq D \leq 10^7$ ly. The longest distance exceeds the distance to the Andromeda galaxy. At greater distances, twice the event horizon $2t_H$ (the dashed line) is a good approximation to that excess MECT.

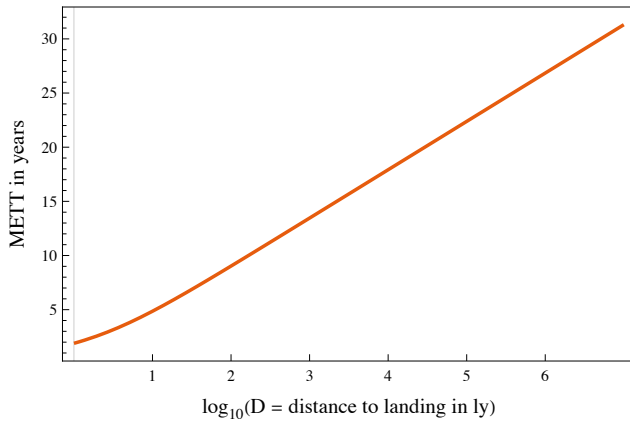


Figure 6: A repeat of Fig.5 for the traveler's time (METT). The canonical-mission METT falls well within a typical single human lifetime even at the greatest distance shown (10^7 ly).

$D = 1000$ ly will have received, at the instant of landing at the destination, ~ 1.9 yr of transmissions from the origin (as measured by the origin's coordinate clock) during a ~ 13.5 yr journey (as measured by the spacecraft's onboard traveler's clock). Thus the crew perceives that they have lost visibility into ~ 11.6 yrs of current events at the origin during their journey. Thereafter the communication from the origin will stream in real-time since

both transmitter and receiver are at rest in the same inertial frame S . Thus the crew will, after landing, be kept up to date with events at the origin as they happen, although ~ 11.6 yr after the fact according to their own traveler's clock. Any denizens at the destination will, in contrast, have the perception that their knowledge of events at the origin is 1000 yr after the fact, which is dramatically greater.

The downlink (direction $C \Rightarrow O$) is very different due to the relatively rapid advance of the coordinate-time. Photons emitted from the spacecraft will arrive at the origin with an x_c/c propagation delay as measured by the origin's coordinate clock, which becomes large for large D .

Example: Continuing the last example, at the origin, news of a successful landing will be delayed for ~ 2002 yrs following the spacecraft launch, which amounts to many generations for a human population. During those intervening centuries, ~ 13.5 yrs of transmissions from the spacecraft will have been slowly received, hopefully serving to maintain awareness of (and interest in) the mission and its outcome. Thereafter, after landing the origin will receive real-time transmissions from the spacecraft, albeit with the perception that they are arriving

$$\sim (2002 - 13.5) = 1988.5 \text{ yr}$$

after the fact.

Rather than communicate back to the origin, an alternative scenario for the spacecraft would be to immediately turn around and travel back to the origin. This would effectively implement time travel ~ 2004 yr into the future, at the expense of ~ 27 yr total elapsed traveler's time.

A general conclusion of the last examples is that the impact of effects like propagation delay and time horizon is minimal for the spacecraft payload in isolation, largely due to compensating relativistic time-dilation effects. However, the impact of these conditions on denizens of the origin and destination is great, and as will be seen (see §5.6), all parties encounter severe obstacles to two-way communication among themselves.

5.5. One-way communication: Clock images

The method of calculating the clock image function (see §2.1) from two trajectories is illustrated in Fig.7. The trajectories are plotted with respect to inertial frame S , and photon trajectories are plotted as unit-slope dashed lines. Each photon trajectory that intersects the two traveler's trajectories in the direction $\mathcal{A} \Rightarrow \mathcal{B}$ defines the clock image $\tau_b = \Psi_{\mathcal{A} \Rightarrow \mathcal{B}}(\tau_a)$ for the pair of traveler's times $\{\tau_a, \tau_b\}$ at the intersection with that photon trajectory.

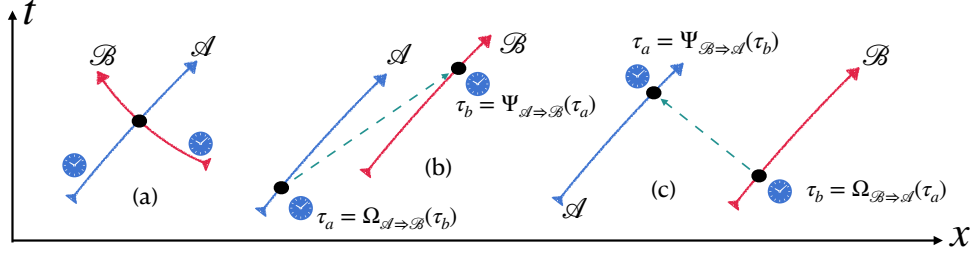


Figure 7: Illustration of the clock image functions for photon transfer between traveler \mathcal{A} with traveler's clock τ_a and traveler \mathcal{B} with traveler's clock τ_b with specified spacetime trajectories represented relative to a common inertial frame S . For the degenerate case of an origin or destination at rest, the corresponding trajectory will be vertical. A photon trajectory in S which intersects both trajectories creates a mapping $\tau_a \Rightarrow \tau_b$ which can be represented by a clock image function $\Psi_{\mathcal{A} \Rightarrow \mathcal{B}}(\cdot)$, as well as a mapping $\tau_b \Rightarrow \tau_a$ which can be represented by an inverse function $\Omega_{\mathcal{A} \Rightarrow \mathcal{B}}(\cdot)$. Note that one or both of the travelers may be at rest (say at the origin or destination), and for such a traveler the trajectory is vertical (with $\tau \equiv t$ within an arbitrary initialization). (a) If the trajectories intersect at some point in spacetime, the instantaneously contiguous traveler's clocks can be directly compared, and if desired initialized to achieve synchronization. For communications this is an uninteresting degenerate case. (b) A photon trajectory in the $+x$ direction. (c) A photon trajectory in the $-x$ direction.

Over the course of a mission there will be a considerable time-warping of the time base of the received signal transmissions in relation to the transmitter time axis (see §5.7). This is manifested by the clock image functions shown in Fig.8 and Fig.9 for a range of launch-landing distances, and for an uplink from origin to spacecraft and downlink from spacecraft to origin.

On the uplink $O \Rightarrow C$ shown in Fig.8, there is a sudden increase in the uplink clock image $\Psi_{O \Rightarrow C}$ at the event horizon t_H because photons will no longer intercept the spacecraft trajectory during the acceleration phase and thus delay their arrival at the spacecraft to the deceleration phase. Post-landing $\Psi_{O \Rightarrow C}$ becomes linear with unit slope since the two clocks increase in lockstep. On the downlink $C \Rightarrow O$ shown in Fig.9 this transition is more gradual, because the photon trajectory is oblique (rather than nearly tangent) to the spacecraft trajectory, but $\Psi_{O \Rightarrow C}$ is exponentially larger (requiring a log plot) since the origin clock does not benefit from time dilation. Thus the photon arrival latency (as observed by the local clock) is exponentially larger on the downlink. As with the uplink, post-landing $\Psi_{C \Rightarrow O}$ becomes linear.

5.6. Two-way communication: Query-response latency

Much can be accomplished by one-way telemetry from spacecraft to origin (for example monitoring of the status of mechanical systems or human crew) and a stream of current events from the origin to the spacecraft. However, if the

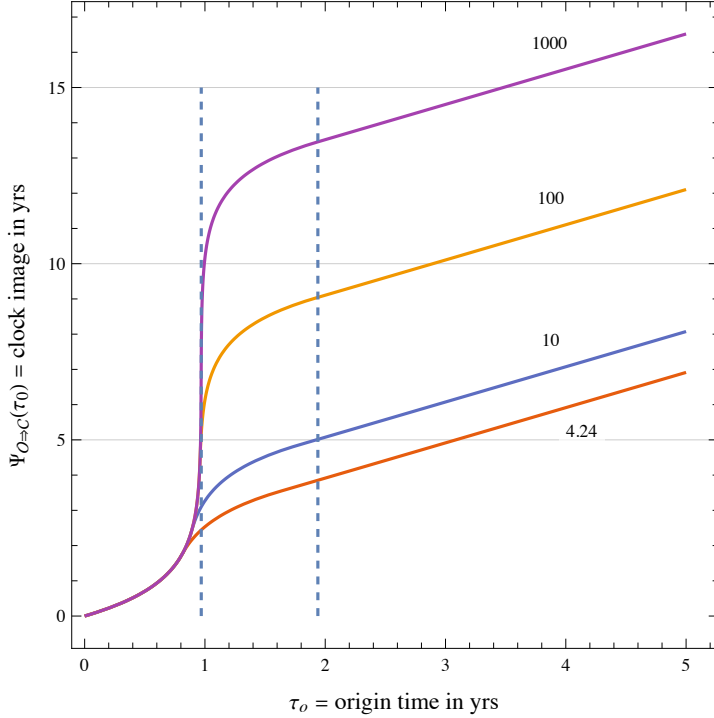


Figure 8: A plot of the clock image $\Psi_{O\Rightarrow C}(\tau_o)$ in years for photon transfer from origin to spacecraft, for a canonical 1-g mission. The vertical dashed lines mark the event horizon t_H and twice the event horizon $2t_H$, which are, respectively, upper bounds on the first half and entirety of the spacecraft cruise phase. Beyond $\sim 2t_H$ the clock image is linear with unit slope because the spacecraft is at rest at the destination. Both horizontal and vertical scales are linear (rather than logarithmic), reflecting the relatively short METT experienced by the spacecraft as well as the relatively short interval before the event horizon is reached at the origin (beyond that, transfer has to await the second half of the cruise phase or following landing). In practical terms, a reasonable delay is achieved for a relatively short time interval following launch. The different curves show the clock image function for different distances $D \in \{4.24, 10, 100, 1000\}$ ly to the destination, with an expansion in METT for the longer distances.

spacecraft is not to be totally autonomous, there is need for two-way communication. This can take the simple form of a query followed by a response to that query (see §2.3.2). In the case of a ‘conversation’, a query followed by a response followed by another query following up on that response, these query-responses repeated indefinitely, might occur. Such conversations are especially useful to human astronauts in maintaining a social connection with family and friends.

5.6.1. Indefinite constant self-acceleration mission

When the self-acceleration continues indefinitely, there are only two query-response latencies of interest, $\mathfrak{L}_{O\Leftarrow C}$ and $\mathfrak{L}_{C\Leftarrow O}$. The values are determined in

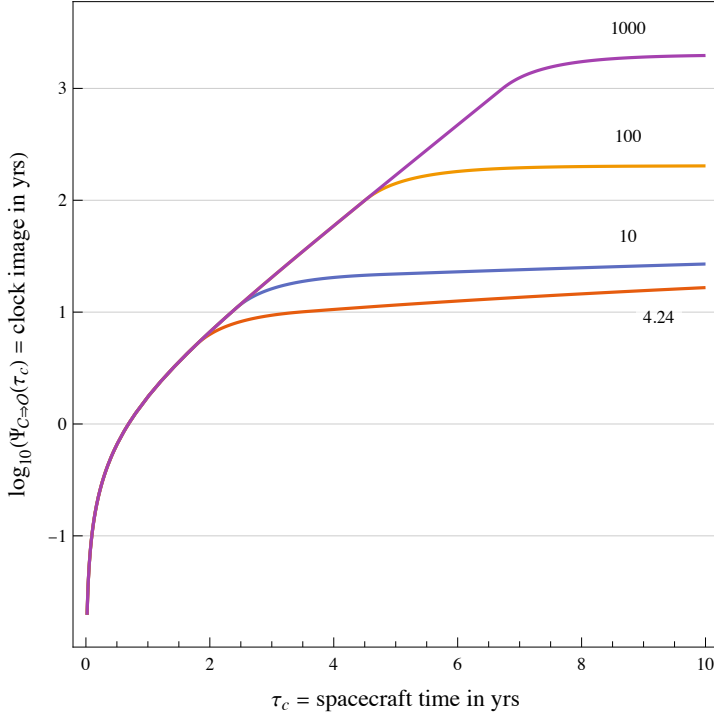


Figure 9: The clock image $\Psi_{C \Rightarrow O}(\tau_c)$ for a photon transfer from a spacecraft to origin. All the conventions of Fig.8 are repeated, except the direction of photon transfer is reversed. The image axis is now logarithmic (in contrast to Fig.8) because photon transfers from the spacecraft now persist over a much longer period (reflecting $\text{MECT} \gg \text{METT}$).

§6.6 and illustrated in Fig.10 for a 1-g mission. Because either the response or the query has to propagate in the same direction as the spacecraft motion, in both cases the traveler's time of a query is limited by the time horizon and latency increases dramatically as that horizon is approached.

5.6.2. Canonical mission

For the canonical mission, which adds the possibility of communicating with the destination, there are six distinctive query-response latencies,

$$\{\mathfrak{L}_{O \Leftrightarrow C}, \mathfrak{L}_{C \Leftrightarrow O}, \mathfrak{L}_{C \Leftrightarrow D}, \mathfrak{L}_{D \Leftrightarrow C}, \mathfrak{L}_{O \Leftrightarrow D}, \mathfrak{L}_{D \Leftrightarrow O}\},$$

but only $\{\mathfrak{L}_{O \Leftrightarrow C}, \mathfrak{L}_{C \Leftrightarrow O}\}$ are quantified here, with the photon trajectories illustrated in Fig.11 and Fig.12. There are also two trivial cases

$$\mathfrak{L}_{O \Leftrightarrow D}[\tau] = \mathfrak{L}_{D \Leftrightarrow O}[\tau] = 2D/c$$

for any traveler's time τ , since O and D are both at rest in S .

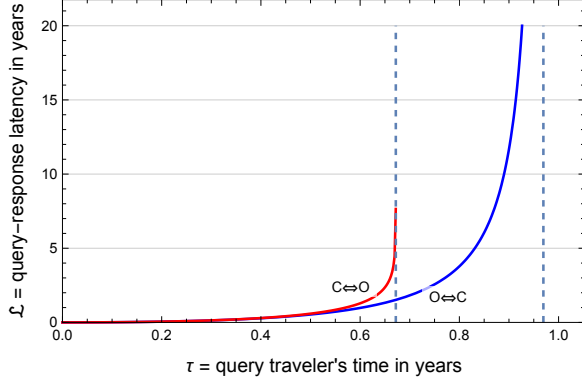


Figure 10: The query-response latencies $\mathfrak{L}_{O\leftrightarrow C}$ and $\mathfrak{L}_{C\leftrightarrow O}$ are compared for an indefinite self-acceleration mission with $\alpha = g$. The opportunity for obtaining a response to a query originating at the origin is limited to the time horizon $\tau_o < t_H$ (shown as the second dashed line), and queries from the spacecraft are more severely limited to $\tau_c < t_H \cdot \log 2$ (also shown as the first dashed line). The latter restriction allows a query to reach the origin soon enough that the response is generated prior to t_H .

$\mathfrak{L}_{O\leftrightarrow C}$ is plotted in Fig.13 and $\mathfrak{L}_{C\leftrightarrow O}$ in Fig.14. There is a rapid increase in the latency until the point at which the spacecraft begins to slow during the deceleration phase of the mission. In the case of $\mathfrak{L}_{C\leftrightarrow O}$, that rapid increase actually occurs prior to the event horizon since the query, following a downlink propagation delay, has to reach O prior to the event horizon.

Save for a period following launch on the order of days or months, the conclusion is that two-way communication becomes at best cumbersome due to large response latencies (on the order of years, decades or centuries, except for missions to relatively nearby targets). Autonomous control of the spacecraft is a must for most of the mission. The implications are profound for a human crew and for humanity back at the origin, because for most of the mission both must rely primarily on one-way streaming of crew status and current events (see §5.5) rather than a conversation.

5.7. Time-warping in streaming communication

The query-response latency captures one common type of communication protocol where one party has a question or comment and the other party responds. Our conclusion is that the latency is impractically large except for communication with the origin for a short period after launch or with the destination for a short period near landing. *Streaming* is a second mode of communication, in which either spacecraft or origin or destination transmits information continuously with no expectation of a response.

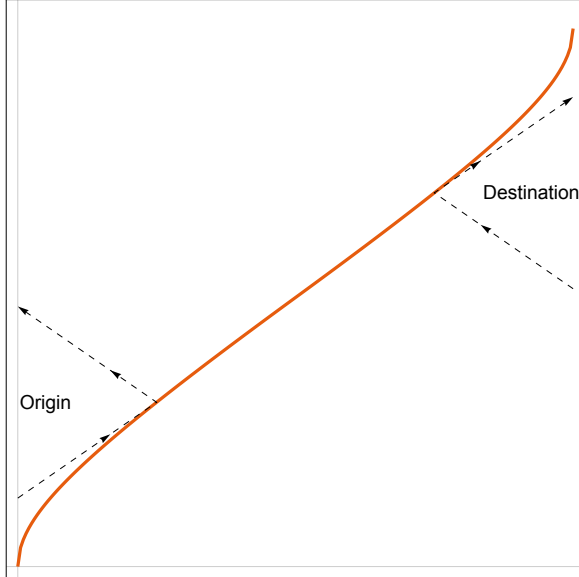


Figure 11: An illustration of the photon trajectories for two-way query-response communication for a canonical 1-g mission with linear axes. Shown are queries originating at the origin and destination, and in each case a response from the spacecraft. The query-response latencies $\mathfrak{L}_{O \leftrightarrow C}$ and $\mathfrak{L}_{D \leftrightarrow C}$ are generally very large (multiple years) unless the query is generated shortly after launch or shortly before landing respectively. The query and the response contribute equally to this latency.

Example: The origin can transmit a continuous stream of sports programming to entertain human astronauts (see §5.7), or the spacecraft can transmit a webcam image of activity onboard the spacecraft back to the origin.

Of course achieving sufficiently high data rates to support reasonable program fidelity is assumed. (Low data rates may limit the fidelity of the streamed material. To improve that fidelity there is the option to stretch the transmission out in time and then transmit it at a lower data rate.) Subject to this limitation, streaming is more practical than query-response communication during the bulk of the cruise phase in that the inevitable propagation delay should not disturb the quality of the viewing experience at the time of reception.

In streaming it is natural to consider a continuous-time transmit and receive signal waveform $s[\tau]$ representing the signal intensity (average rate of photon emissions or detections) vs time. In one common form of modulation, the underlying data is represented by a variation of that intensity. (There are other less energy-efficient modulation techniques that modulate phase and/or wavelength, typically in the context of heterodyne as opposed to photon-counting detection.) The effect of accelerated motion is a nonlinear ‘warp’ in the timebase τ of the

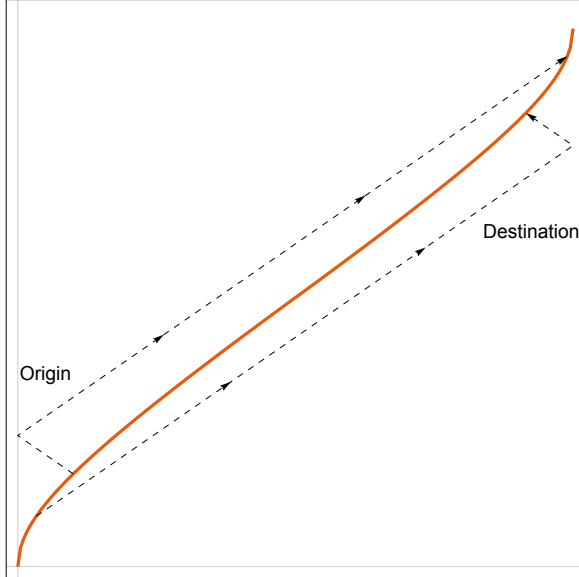


Figure 12: A repeat of Fig.11 for queries from the spacecraft to the origin and to the destination, also with linear axes. Again the latencies $\mathfrak{L}_{C \leftrightarrow O}$ and $\mathfrak{L}_{C \leftrightarrow D}$ are generally very large (multiple years) unless the query is generated shortly after launch or shortly before landing respectively. The photon propagation in the direction of the spacecraft trajectory contributes disproportionately to latency in both cases.

waveform $s[\tau]$ between the transmitter and receiver.

When streaming to or from the spacecraft, it is evident from Fig.4 (and keeping in mind that coordinate time is greatly expanded relative to the spacecraft traveler’s time) that there is a significant expansion or contraction of a streaming program’s duration. In the case of streaming to or from the origin (the only case considered here), a streaming program’s duration is expanded from transmitter to receiver in both directions:

- From origin to spacecraft this is due to the time horizon limitation (which is less than the METT) on total transmit time.
- From spacecraft to origin this is due to the expansion in coordinate time relative to spacecraft traveler’s time (since $MECT \gg METT$).

In both cases, if the program is streamed in “real time” at the transmitter, it is not only delayed (due to propagation delay) but also has an expanded duration at the receiver. If desired it can be stored at the receiver and subsequently played back at a higher speed (to return to real time). This time expansion is due to very different physical effects in the two directions. For $O \Rightarrow C$ this is due to the

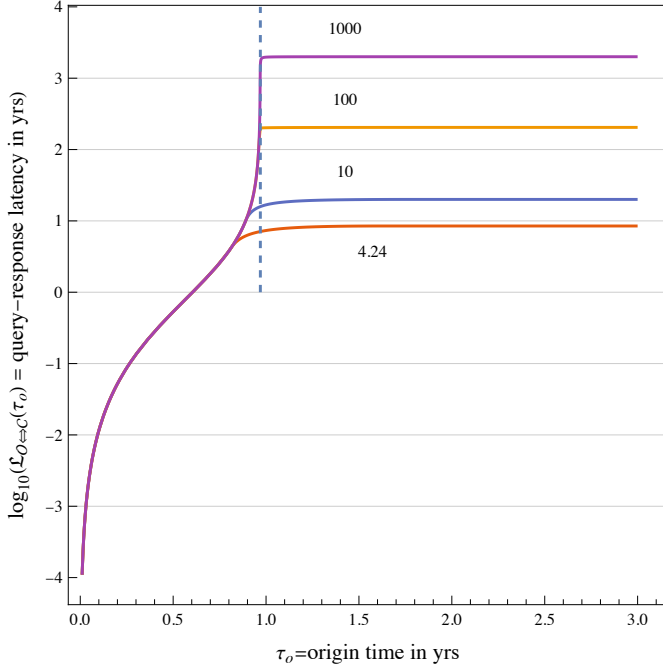


Figure 13: A plot of the query-response latency $\mathfrak{L}_{O \Leftrightarrow C}$ in years for queries sent from the origin to the spacecraft for a canonical 1-g mission. The photon trajectories were illustrated in Fig.11). The horizontal axis is the time after launch ($\tau_o = 0$) that a query to the spacecraft is originated at the origin, and the vertical axis is the resulting query-response latency. Only a very small fraction of the total MECT is plotted, especially at the longer distances. The vertical axis is logarithmic, reflecting the very large $\mathfrak{L}_{O \Leftrightarrow C}$ following the event horizon t_H (shown as a vertical dashed line). Queries sent following t_H result in much greater latency since the query does not reach the spacecraft until the second half of its cruise phase. The different curves show $\mathfrak{L}_{O \Leftrightarrow C}$ for different distances $D \in \{4.24, 10, 100, 1000\}$ ly to the destination, with longer distances resulting in greater $\mathfrak{L}_{O \Leftrightarrow C}$ beyond the event horizon due to the longer duration of acceleration (as opposed to deceleration).

rapidly increasing propagation delay experienced by photons as the event horizon is approached (this is a classical effect). For $C \Rightarrow O$ this is a manifestation of the relatively slow evolution of the traveler's time τ_c relative to the coordinate clock t_o , which is a manifestation of relativistic time dilation (this is directly related to the observation that $\text{METT} \ll \text{MECT}$).

For the streaming of programs of finite length (hours rather than years), this motion-induced time warp has minimal variation within the program duration. The timebase expansion can then be approximated by the derivative of the receiver local time with respect to the transmitter local time referenced to a specific traveler's time τ_c at the spacecraft, and assuming that the result is constant over time intervals of interest. This derivative is evaluated in §Appendix B.4 for the

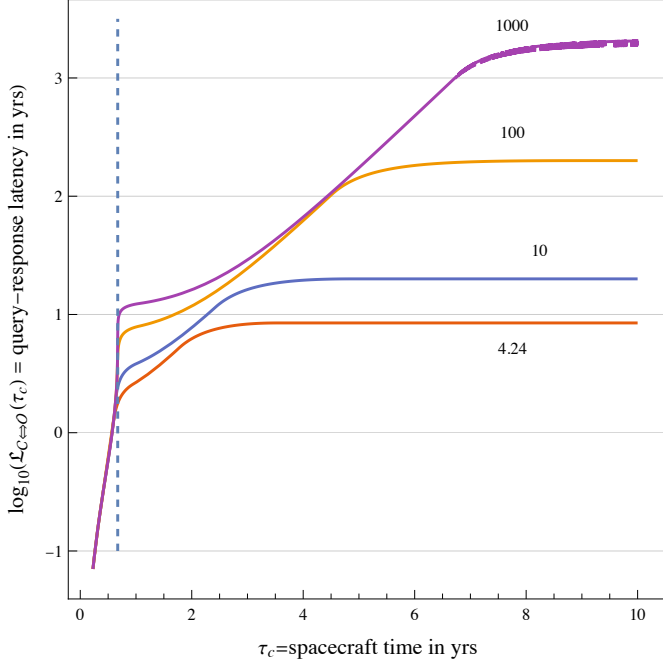


Figure 14: A plot of the query-response latency $\mathfrak{L}_{C \Rightarrow O}$ in years for queries sent from the spacecraft to the origin for a canonical 1-g mission. The photon trajectories were illustrated in Fig.12. All the conventions of Fig.13 are repeated, except the direction of photon transfer is reversed. Thus the horizontal axis is the traveler's time τ_c at which the spacecraft originates the query, and the vertical axis is the logarithm of the resulting query-response latency as measured by that same traveler's time. The vertical dashed line is at $\tau_c = t_H \cdot \log 2$, which is the τ_c for which a photon emitted from the spacecraft reaches the origin at the event horizon $\tau_o = t_H$ (see Eq.(17b)). This is the point at which responses begin to experience much larger delays (see Fig.8).

simpler indefinite self-acceleration case, and found to be

$$\left. \frac{d\tau_c}{d\tau_o} \right|_{O \Rightarrow C} = \left. \frac{d\tau_o}{d\tau_c} \right|_{C \Rightarrow O} = \frac{\Psi_{C \Rightarrow O}[\tau_c]}{\Omega_{O \Rightarrow C}[\tau_c]} = e^{\tau_c/t_H}. \quad (8)$$

The timebase is expanded (rather than contracted), and is identical in the two directions, when referenced to the same instant from the spacecraft perspective, in spite of the distinctive physical processes at work. It increases exponentially with the spacecraft traveler's time τ_c due to the continuous increase in speed under constant acceleration.

Example: The origin O streams a football match to the spacecraft C , and the spacecraft streams back a webcam video of the astronauts watching the match so that the controllers at the origin can gain vicarious enjoyment from watching the astronauts' reaction to the goals.

We are interested in the timing of this interaction. The appropriate timebases are the local clocks at \mathcal{O} and \mathcal{C} that govern the streaming timebases in the respective directions. Assume that these clocks are initialized so that $\text{MECT} = t_o$ at \mathcal{O} and $\text{METT} = \tau_c$ at \mathcal{C} .

Consider the case where the match video arrives at \mathcal{C} following two years of 1- g self-acceleration, or $\tau_c=2$ yr, and the webcam video is simultaneously streamed back. What are the times of transmission and reception of these streams at the origin? These times are revealed by the appropriate clock images, which are derived later in §6.6, with the result

$$\mathcal{O}\Rightarrow\mathcal{C}: t_o = \Omega_{\mathcal{O}\Rightarrow\mathcal{C}}[\tau_c=2 \text{ yr}] = 0.846 \text{ yr} = 309 \text{ days} \quad (9a)$$

$$\mathcal{C}\Rightarrow\mathcal{O}: t_o = \Psi_{\mathcal{C}\Rightarrow\mathcal{O}}[\tau_c=2 \text{ yr}] = 6.66 \text{ yr}. \quad (9b)$$

Although both directions of streaming are concurrent at the spacecraft, at the origin the $\mathcal{C}\Rightarrow\mathcal{O}$ webcast is delayed by 5.8 yr relative to the $\mathcal{O}\Rightarrow\mathcal{C}$ match. The controllers at the origin have to wait multiple years to observe the astronauts' reaction.

What is the timebase expansion of the two streaming programs? Applying Eq.(8), the expansion in $\mathcal{O}\Rightarrow\mathcal{C}$ happens to be the same as the expansion $\mathcal{C}\Rightarrow\mathcal{O}$. (Again this assumes the spacecraft's reception of the match and the spacecraft's transmission of the webcast are simultaneous.) In both cases this expansion is a factor of 7.87. (The ratio of Eq.(9b) to Eq.(9a) also evaluates to 7.87, which is also anticipated in Eq.(8).) Thus a one-hour football match would be expanded to 7.87 hours at the receiver. If the match video is played back as it is received, it would appear to be running in slow motion. To make the presentation more natural for the astronauts, the streamed match could be stored and subsequently played back at its original speed (which is 7.87 times faster than it was received). Identical logic applies independently to the spacecraft's webcast as it is received by the controllers.

Similarly, in streaming to and from the destination, it can be shown that the timebase contracts (rather than expands), is the reciprocal (decreases exponentially), and is identical in the two directions $\mathcal{C}\Rightarrow\mathcal{D}$ and $\mathcal{D}\Rightarrow\mathcal{C}$. Although these symmetries generalize to an arbitrary spacecraft trajectory, they are attributable to \mathcal{O} and \mathcal{D} both being at rest in S and do not apply when they are in motion.

5.8. Communication between two spacecraft

We can imagine two spacecraft with the same acceleration profile, but launched at different times, for example in an alien-world colonization scenario. In that

case it is interesting to consider the possibilities for communication between this pair of spacecraft.

Suppose that there are two spacecraft $C1$ and $C2$ launched in that order, so the ordering of spacecraft versus distance is

$$O \rightarrow C2 \rightarrow C1 \rightarrow \mathcal{D}.$$

Thus during their respective cruise phases, their trajectories are illustrated in Fig.15. The traveler's times aboard the two spacecraft initialized to $\tau_{c1} = \tau_{c2} = 0$ at their respective launch times, so that they measure the METT for each spacecraft.

Our immediate concern is exploration of the photon exchange between $\{C2, C1\}$ in both directions. As illustrated in Fig.15, photon exchange $C2 \Rightarrow C1$ is feasible as long as the launch time of $C2$ falls within $0 < t_o < t_H$ (as it does in this case). However, the photon emission time is limited by the event horizon of $C1$, after which there is a communication blackout.

The clock images for communication in both directions are illustrated in Fig.16 and Fig.17 for a $C2$ launch coordinate time $t_o = \epsilon t_H$ where $0 < \epsilon < 1$ (see §Appendix B.3). The query-response latencies for two-way communication between $C2$ and $C1$ are illustrated in Fig.18 and Fig.19.

5.9. Role of acceleration magnitude and duration

The canonical mission of Fig.1 makes the assumption that acceleration magnitude is time-invariant during the entire travel time from launch to landing. Having developed a complete picture of one-way image and two-way query-response latency, two modifications that can be made in the interest of easing the restrictions on communication can be considered. One is reducing the acceleration and deceleration time durations, thereby introducing an intermediate 'ballistic' interval during which the spacecraft speed is constant. The second is reducing the acceleration magnitude α (thereby increasing t_H). Neither will make a meaningful change in MECT, and hence neither change would have significant impact on the origin's awareness of landing, nor on response latencies. However, these modifications would have a significant effect on one-way uplink communication to the spacecraft by lengthening the event horizon t_H (allowing longer communication with the origin during the acceleration phase) and/or by earlier termination of the acceleration phase (allowing uplink signals transmitted past the event horizon to be received earlier). Employing a combination of larger t_H and a shorter acceleration phase could allow an extension of the event horizon past the acceleration phase altogether.

A significant impact of either of these modifications would be in increasing the METT, with the resulting adverse implications for resources aboard the spacecraft and the required lifetime of equipment and crew. The greater mass

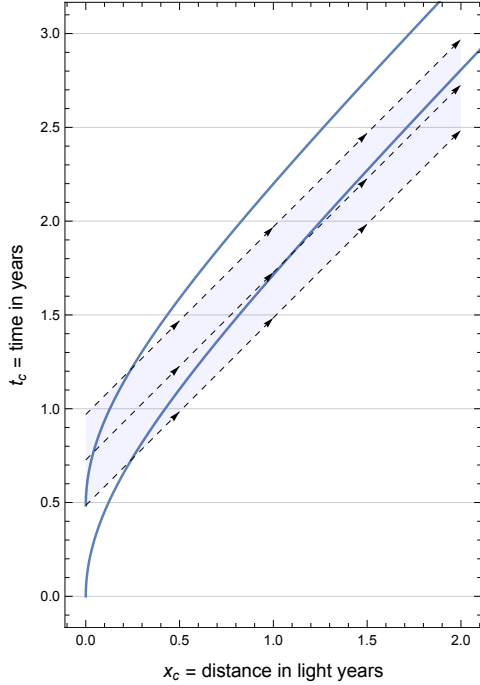


Figure 15: A plot of the trajectories of two spacecraft launched from the origin O at different times, each with indefinite 1- g self-acceleration. One spacecraft (which is traveler $C1$) is launched at $t_o = 0$ and the other (which is traveler $C2$) is launched at $t_o = 0.5 \cdot t_H$. Also shown as dashed lines are the trajectories of a photon emitted from the origin at three coordinate times $t_o \in \{0.5, 0.75, 1\} \cdot t_H$ in the $+x$ direction. The shaded area represents the ensemble of photon emission times from $C2$ which intersect the trajectory of $C1$ (and hence can be detected by $C1$). This represents a finite interval beginning at the instant of launch of $C2$.

associated with greater resources would be compensated by lower mass devoted to spacecraft propulsion. The human crew would devote more of their lifetime to the cruise phase (and commensurately less to the post-landing) experience.

6. Analysis

Relativistic effects can generally be neglected in the case of spacecraft missions within our Solar System, at least when chemical spacecraft propulsion is employed and the speeds are relatively low compared to light-speed c . This implies that the Newtonian theory of gravity and a single universal measure of coordinate time in the predication of spacecraft trajectories and communication latencies is suitably accurate. This approach has to be abandoned for interstellar missions, where the full General Theory of Relativity (GR) [2] could be adopted. In this paper the ‘empty-space’ approximation is utilized, in which the spacecraft trajectory is

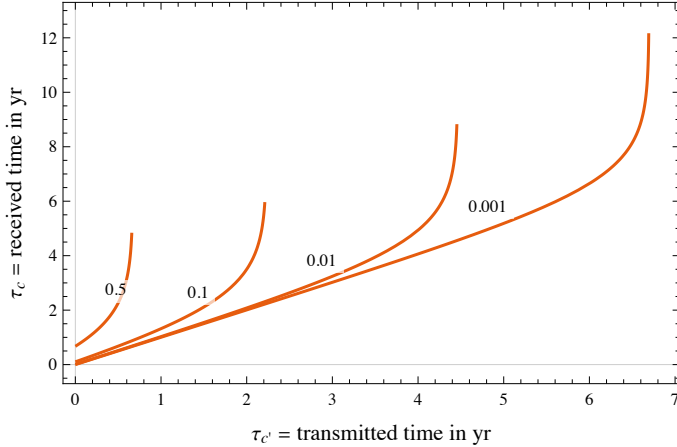


Figure 16: The clock image $\Psi_{C2 \Rightarrow C1}$ for photon exchange from $C2$ to $C1$ is plotted. Two spacecraft $C1$ and $C2$ are launched in that order, so that photon propagation is in the same direction as the spacecraft trajectories. Both spacecraft are assumed to have indefinite 1- g acceleration, and the traveler's times $\{\tau_{c1}, \tau_{c2}\}$ each measure METT for their respective spacecraft ($\tau_{c1} = \tau_{c2} = 0$ at launch). The different curves represent $\epsilon \in \{0.1, 0.5, 0.9\}$, where the later-launch is delayed by ϵt_H relative to the earlier launch. The time τ_{c1} for photon detection by $C1$ occurs increasingly late in its trajectory as ϵ increases. There is a limit $-t_H \cdot \log \epsilon$ on the emission time τ_{c2} that falls within the time horizon of $C1$. The image $\Psi_{C2 \Rightarrow C1}$ is unbounded toward the end of that interval.

determined entirely by its own propulsion, neglecting the effects of gravity from astronomical bodies including the origin and destination. This is the standard approach for development of the relativistic spacecraft equation [3, 4], and relies on the simpler (and more analytically tractable) Special Theory of Relativity (SR).

There are numerous resources for studying SR, including some excellent textbooks [5, 6, 7]. We follow an alternative approach and notation to the development of SR originating in [1], which (it was argued) is more appropriate for engineering applications such as interstellar travel (as opposed to scientific applications). In particular the perspective of the traveler (accelerated observer) was adopted in place of the usual denizen (inertial) observer universally adopted in physics, starting with Einstein's initial formulation. This alternative development greatly simplifies the derivation of trajectories involving acceleration, and is consistent with the universal practice of relying on clocks carried by spacecraft. This approach was inspired in part by earlier pedagogical innovations by Fraundorf [8, 9, 10] and a new derivation of the relativistic spacecraft equation by Walter [11, 12]. The notion of a clock image, which forms the basis of the communication latencies developed here, was introduced in [1].

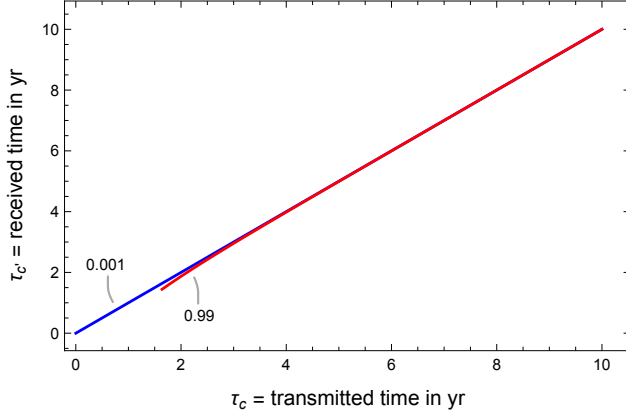


Figure 17: Fig.16 is repeated for photon exchange from an earlier-launched $C1$ spacecraft to a later-launched spacecraft $C2$, with photon propagation in the opposite direction to the spacecraft trajectories. The clock image is $\Psi_{C1 \Rightarrow C2}$ and for this case a communication blackout never occurs. The earliest photon emission time τ_{c1} by $C1$ is $t_H \cdot \log(1 + \epsilon)$, since earlier emissions would arrive prior to the launch of $C2$ (recall that $C2$ is launched later than $C1$). Later in $C1$'s trajectory, ϵ has minimal impact on $\Psi_{C1 \Rightarrow C2}$.

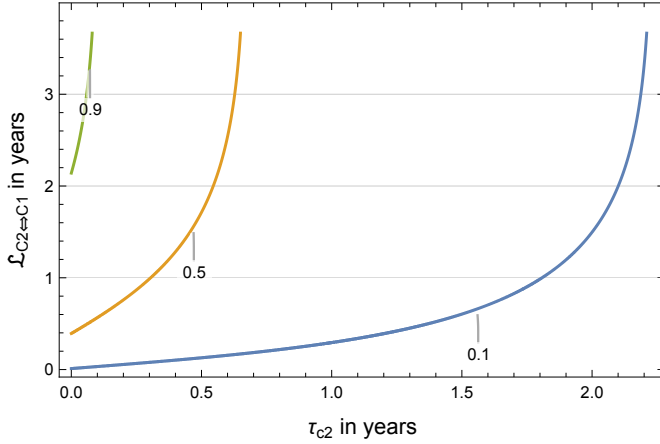


Figure 18: The query-response latency $\mathfrak{L}_{C2 \Leftrightarrow C1}$ for a query initiated by the later-launched rocket $C2$ to the earlier-launched rocket $C1$ is plotted for the same assumptions as in Fig.16. Queries can be initiated by $C2$ immediately following launch, but receiving a response is only possible for an interval $0 < \tau_{c2} < -t_H \cdot \log \epsilon$ following launch. Toward the end of that interval $\mathfrak{L}_{C2 \Leftrightarrow C1}$ becomes unbounded.

Most relativistic spacecraft derivations assume that the propulsion is based on a fixed-rate consumption of a propellant carried by the spacecraft, in which case the force exerted on the spacecraft will be constant. As the mass of the spacecraft

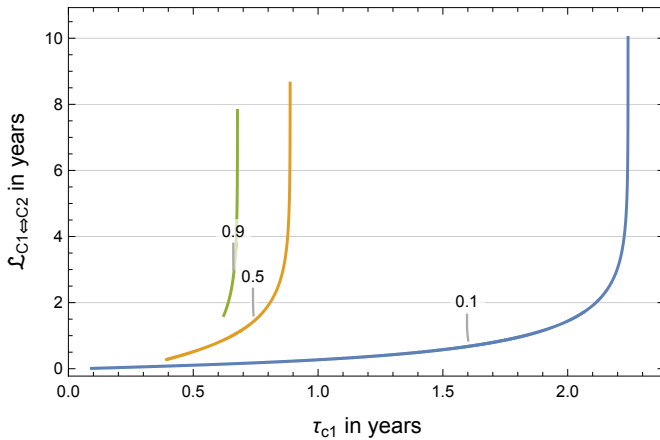


Figure 19: The query-response latency $\mathcal{L}_{C1 \leftrightarrow C2}$ for a query initiated by the earlier-launched spacecraft $C1$. This is a repeat of Fig.18 for a query in the opposite direction. Both the earliest and latest such query is constrained. The earliest query arrives at $C2$ at the instant of its launch. There is also a latest such query time $t_H \cdot \log(\epsilon + 1/\epsilon)$ that allows for a response from $C2$ to reach $C1$. This is because that response must be initiated early enough to fall within the time horizon of $C1$. As the time horizon is reached, $\mathcal{L}_{C1 \leftrightarrow C2}$ grows without bound.

decreases, the self-acceleration thereby increases. In contrast, the canonical mission considered here assumes that the self-acceleration of the spacecraft is fixed. This would require that the rate of fuel consumption start out high to compensate for the higher initial fuel mass, and decrease during the mission. Alternative versions of the spacecraft equation are derived and compared in [1]. Here we do not take propulsion challenges into account, but rather make the ‘empty-space constant self-acceleration’ simplifying assumption in order to focus our efforts on understanding the communication timing issues in a simple context. Our methods readily extend to more complicated mission scenarios.

6.1. Map and two clock metaphor

A map and two-clock metaphor [1] forms the basis for the following. The kinematic variables used in this metaphor are summarized in Tbl.2.

A coordinate system to describe the trajectory of a moving body like a spacecraft C is defined relative to an inertial frame S which defines a set of spatial coordinates. Relative to S , any observer \mathcal{R} with fixed spatial coordinates (said to be *at rest*) experiences no acceleration. The coordinates defined by S are called a *map*, in analogy to terrestrial travel, and the position of an observer is called the *map-position*. For the general case a map-position is three-dimensional, but for simplicity here we specialize to the one-dimensional (rectilinear) case. Thus there is a single scalar spatial coordinate, which is labeled r or x . Any body such as C not permanently at rest is called a traveler.

Table 2: Kinematic variables for a 1-D map and two-clock metaphor

Variable	Traveler's version	Coordinate version
Map-position	r	x
Time	τ	t
Time-speed		$\gamma = t' = \frac{dt}{d\tau}$
Map-speed	$w = r' = \frac{dr}{d\tau}$	$u = x' = \frac{dx}{dt}$
Self-acceleration	α	
Map-acceleration	$w' = \frac{dw}{d\tau}$	$u' = \frac{du}{dt}$

There are two types of clocks of interest. The traveler's clock (carried along with C), is the clock of interest in the context of interaction (such as communication) among two or more travelers, and measures traveler's time τ (as was described in §2). Any clock at rest in S is called a coordinate clock, because it measures *coordinate time* denoted by t . Traveler and coordinate clocks advance at different rates, excepting the degenerate case of a traveler temporarily or permanently at rest relative to S . Clock synchronization, the issue of initialization of all clocks, was discussed in §4.3.

Kinematic variables quantify the motion of travelers, and for our purposes constitute map-position as well as the map-speed and map-acceleration measured at the same map-position. SR offers a complete model of kinematics, for accelerated bodies as well as inertial, in the absence of gravitational influence. Since map-speed is the derivative of map-position, and map-acceleration is the derivative of map-speed, both relative to an appropriate definition of time, there are two distinct sets of kinematic variables. The traveler's set, measured relative to τ , is denoted by $\{\tau, r, w, w'\}$, where w' denotes the derivative of w with respect to τ . Similarly the coordinate set $\{t, x, u, u'\}$ is measured relative to t .

In addition to $\{w', u'\}$, there is a third measure of acceleration α measured by an accelerometer carried aboard the spacecraft, and called the *self-acceleration*. Any accelerometer must implicitly incorporate a measurement of time, and the appropriate clock for this purpose is the traveler's clock (which is carried along with that accelerometer as part of the traveler's payload). Thus α is unambiguously measured relative to traveler's time τ (there is no coordinate-time version). In general the three forms of acceleration $\{w', u', \alpha\}$ possess different numerical values at any instant of time. The coordinate map-acceleration u' is of no concern in the following.

Finally, the *time-speed* γ (called the *Lorentz factor*) measures the rate of advance of a coordinate clock t relative to a traveler's clock τ situated at the

same position.

6.2. Time dependence of kinematic variables

Since there are two distinct time measurements of interest, to keep things straight we exercise care in expressing the time dependence of kinematic variables. There are two kinematic variables that are unaffected by the choice of S , and depend only on τ and not t : These are τ itself and self-acceleration $\alpha[\tau]$. The other kinematic variables not only have a coordinate-time version, but more fundamentally these variables are affected by the choice of S . Since it is frame-invariant, τ is preferred as the fundamental timebase for accelerated motion, and the traveler’s time kinematic variables are written as $\{\tau, \gamma[\tau], r[\tau], w[\tau], w'[\tau]\}$. This kinematic description is also practical because a traveler is assumed to carry a clock measuring τ , and the traveler is normally navigationally aware of its own position $r[\tau]$.

This is so simple and clean, it is reasonable to ask “in the communications context, what purpose is served by a coordinate-time description of kinematics?” A fundamental postulate of SR is that the speed of light c is invariant to the choice of inertial frame S . The interaction among different travelers is based on photon exchange, and the propagation delays for photons are defined in terms inertial frame S and coordinate time t . Thus for us to quantify photon-transfer interactions, for each traveler emitting or detecting a photon we must know its traveler’s time τ and map-position $r[\tau]$ at that instant, but also the associated coordinate time at that map-position and instant of time, which we write as $t[\tau]$. It would be unusual for there to be an actual physical clock at rest at that map-position, so typically this coordinate clock is *notional* rather than physical. The entire set of kinematic variables can thus be written as $\{t[\tau], x[t[\tau]], u[t[\tau]], u'[t[\tau]]\}$. For purposes of photon transfer timing calculations (the focus of this paper), the only coordinate variable needed is $t[\tau]$, since map-position is conveniently specified by $r[\tau]$.

The calculations establishing all the useful kinematic variables proceeds in the following sequence:

$$\alpha[\tau] \rightarrow w'[\tau] \rightarrow w[\tau] \rightarrow r[\tau] \tag{10a}$$

$$w[\tau] \Rightarrow \gamma[\tau] \rightarrow t[\tau] . \tag{10b}$$

Each ‘ \rightarrow ’ represents the solution to a first-order differential equation (DE) given in Tbl.2 (with the exception of $\alpha[\tau] \rightarrow w'[\tau]$, which is noted below), and the single ‘ \Rightarrow ’ is a functional relation also noted below. All kinematic variables follow from knowledge of $\alpha[\tau]$, which is the input. The final outcome $\{r[\tau], t[\tau]\}$ is everything needed for the photon transfer propagation delay calculations that enter into clock images and the resulting query-response latencies.

6.3. Kinematic variable solutions

The role of time-speed $\gamma[\tau]$ becomes evident when the two versions of map-speed are compared. Applying the chain rule of differentiation,

$$w[\tau] = r'[\tau] = x'[t[\tau]] \cdot t'[\tau] = u[t[\tau]] \cdot \gamma[\tau]. \quad (11)$$

Thus $\gamma[\tau]$ directly relates the two map-speeds. The $w[\tau] \Rightarrow \gamma[\tau]$ relation in Eq.(10b) is [1]

$$\gamma[\tau] = \sqrt{1 + w[\tau]^2/c^2}. \quad (12)$$

If S is changed for any reason, both $\gamma[\tau]$ and $w[\tau]$ are affected as a result, but their frame-invariant relationship in Eq.(12) is preserved.

Relation Eq.(12) has profound implications for interstellar travelers (analogous to $E = mc^2$ for energy and propulsion) because it directly relates motion and time. In particular, since for a moving body $1 < \gamma[\tau]$, it follows that τ always advances more slowly than $t[\tau]$, and the larger the map-speed, the larger this *time-dilation* effect. A natural question is “what is the asymmetry that causes this disparity to always occur in the same direction”. One simple answer is that a measurement of the traveler kinematic variables expressed in terms of traveler’s time can be accomplished using the single traveler’s clock carried by the traveler, but measuring such variables expressed in terms of coordinate time requires two or more coordinate clocks.

Eq.(12) and Eq.(11) together imply that ($|u[t[\tau]]| < c$), leading to the common perception that objects cannot travel faster than light. This is at best an incomplete statement when applied to interstellar travel, because spacecraft self-aware of their own motion employing their own clock as the basis of observations see no such limitation on speed (since $|w| \gg c$ is possible). The spacecraft’s perception of super-luminance (travel faster than light-speed) is attributable to its traveler’s clock advancing more slowly. There is no inconsistency since a traveler’s clock is incapable of measuring photon speed. Since $|u| < c$ a traveler’s clock as observed in S necessarily travels slower than a photon, and thus could measure either the time of a photon’s emission or the time of that same photon’s detection, but never both.

The $\alpha[\tau] \rightarrow w'[\tau]$ DE in Eq.(10a) is given by [1]

$$w'[\tau] = \gamma[\tau] \cdot \alpha[\tau]. \quad (13)$$

After substituting for $\gamma[\tau]$ from Eq.(12), this becomes a first-order DE in $w[\tau]$. This is another frame-invariant relation; that is, both $w[\tau]$ and $\gamma[\tau]$ are affected by the choice of S , but relationship Eq.(13) is not. The self-acceleration $\alpha[\tau]$ is of practical interest for two important reasons:

- Acceleration α relates directly to the force imparted by the propulsion system [11], if propulsion is the cause of the acceleration. (Another possibility is gravity, but that effect is neglected in SR.)
- Acceleration α is that experienced by on-board equipment and material, including biological material, both of which are normally sensitive to and affected by the acceleration magnitude. In numerical examples a time-invariant 1-g self-acceleration magnitude is assumed, because this is consistent with that normally experienced by humans and other biological material originating from Earth.

Since again $1 < \gamma[\tau]$, what follows from Eq.(13) is the profound observation that $|w'[\tau]| > |\alpha[\tau]|$, which is called an *acceleration boost*. That map-acceleration is always greater than self-acceleration is great news for interstellar travelers. Although biological organisms (like humans) have a limited tolerance for high self-acceleration, that intolerance need not limit the map-acceleration. Even better news for interstellar travelers is a positive feedback effect: As $w[\tau]$ grows so does $\gamma[\tau]$, and hence acceleration boost magnitude is amplified without limit for as long as self-acceleration (in the direction of travel) persists. This makes it advantageous to maintain self-acceleration as long as possible (as in the canonical mission assumption, see §5.9), because longer self-acceleration reduces the METT (while its effect on MECT is minimal) and thus reduces the resources (food, water, oxygen, etc) required on the spacecraft, as well as biological aging.

6.4. Trajectory with indefinite self-acceleration

The coordinate-time spacecraft trajectory $\{r_c[\tau_c], t_c[\tau_c]\}$ for constant acceleration and time horizon t_H (see §Appendix B.1) is

$$t_c[\tau_c] = t_H \cdot \sinh(\tau_c/t_H) \quad (14a)$$

$$r_c[\tau_c] = c t_H \left(\cosh(\tau_c/t_H) - 1 \right). \quad (14b)$$

This is consistent with the textbook *hyperbolic trajectory* for a uniformly accelerated body (see Ch.14 of [7]), although here it has been derived in an unconventional way.

Example: Let the units of time be year and the units of distance be light years, and determine the kinematic variables at $\tau_c=2$. The coordinate map-speed is $u=0.968$ (96.8% of c), the traveler's map-speed is $w=3.87$ (387% of c), and the time-speed is $\gamma=4.0$. While the traveler's self-acceleration is $\alpha = g=1.03$, the traveler's map acceleration is $w'=4.13$ ($\gamma=4.0$ times the self-acceleration α).

6.5. Event horizon

Before verifying the event horizon analytically, the interpretation of the phrase “trajectory of a photon” should be clarified. As $u[t[\tau]] \rightarrow c$ we find that $\gamma[\tau] \rightarrow \infty$, which implies that $\tau \rightarrow 0$. Thus, from the perspective of a photon (if indeed it had its own perspective!) we have $\tau \equiv 0$. A photon trajectory cannot be parameterized by τ (as in the case of non-zero mass particles). Rather, a photon trajectory $\{x[t], t\}$ must omit τ altogether. A fundamental postulate of SR is that a photon’s position versus coordinate time obeys the *range equation*

$$t = t_0 + x[t]/c \quad (15)$$

for a photon that is emitted from position $x[0] = 0$ at time $t = t_0$. This expresses the simple concept that the photon travels at speed c from the perspective of observers at rest in inertial frame S . Photon trajectories in previous plots have this special interpretation.

Analytically verifying the time horizon phenomenon follows from comparing two coordinate times:

Spacecraft. When the spacecraft travel time is τ_c , its distance reached is $r_c[\tau_c]$ and the coordinate time at which it reaches this distance is $t_c[\tau_c]$.

Photon. Based on Eq.(15), the coordinate time that a photon emitted from the origin at coordinate time $t_c[\tau_c] = t_H$ arrives at the same distance $r_c[\tau_c]$ is $(t_H + r_c[\tau_c]/c)$.

Substituting from Eq.(14), the difference between these two times

$$(t_H + r_c[\tau_c]/c) - t_c[\tau_c] = t_H \cdot e^{-\tau_c/t_H} > 0 \quad (16)$$

is positive and approaches zero exponentially as $\tau_c \rightarrow \infty$. Thus the photon and accelerated spacecraft trajectories approach one another (but never intersect). The event horizon no longer applies when the spacecraft terminates its acceleration and/or starts decelerating, as illustrated in Fig.20.

6.6. Clock images and query-response latencies

There are two clock image functions (see §5.5) of interest, $\Psi_{O \Rightarrow C}$ and $\Psi_{C \Rightarrow O}$. For trajectory Eq.(14) (see §Appendix B.2),

$$\tau_c = \Psi_{O \Rightarrow C}[\tau_o] = -t_H \cdot \log(1 - \tau_o/t_H), \quad 0 \leq \tau_o < t_H \quad (17a)$$

$$\tau_o = \Psi_{C \Rightarrow O}[\tau_c] = t_H (e^{\tau_c/t_H} - 1), \quad 0 \leq \tau_c. \quad (17b)$$

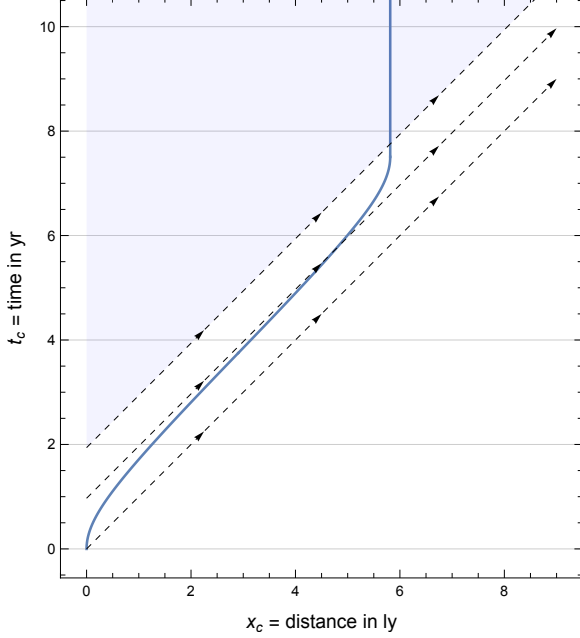


Figure 20: Illustration of the trajectory of a canonical launch-to-landing 1-g mission as defined in Fig.21. The origin to destination distance D is chosen so that the total METT at landing is $\tau_c = 4$ yr (see §7). This is a repeat of Fig.3 with the addition of a deceleration cruise phase. The dashed lines show the trajectories of photons emitted from the origin at $t_o \in \{0, t_H, 2t_H\}$. In this case the spacecraft can detect photon emissions during the interval $\sim t_H < t_o < \sim 2t_H$ during the deceleration, but emissions for $\sim 2t_H < t_o$ can only be detected following landing at the destination. A photon that is emitted from the origin at $t_o = 2t_H$ is detected shortly following landing, so that MECT $\sim (D/c + 2t_H)$.

The domain of $\Psi_{O \Rightarrow C}$ is restricted to the interval between launch and event horizon as expected, whereas the domain of $\Psi_{C \Rightarrow O}$ is only restricted to post-launch, although it grows exponentially. The corresponding inverse clock image functions are

$$\tau_o = \Omega_{O \Rightarrow C}[\tau_c] = t_H \cdot \left(1 - e^{-\tau_c/t_H}\right), \quad 0 \leq \tau_c \quad (18a)$$

$$\tau_c = \Omega_{C \Rightarrow O}[t_o] = t_H \cdot \log\left(1 + \tau_o/t_H\right), \quad 0 \leq \tau_o. \quad (18b)$$

The resulting query-response latencies are (see §Appendix B.2),

$$\mathfrak{L}_{O \Rightarrow C}[\tau_o] = \frac{\tau_o^2}{t_H - \tau_o}, \quad 0 \leq \tau_o < t_H \quad (19a)$$

$$\mathfrak{L}_{C \Rightarrow O}[\tau_c] = -t_H \cdot \log\left(2 - e^{\tau_c/t_H}\right) - \tau_c, \quad 0 \leq \tau_c < t_H \cdot \log 2. \quad (19b)$$

The range of $\mathfrak{L}_{C \leftrightarrow O}$ is more restricted (since $\log 2 \approx 0.69$) because the query has to reach the origin early enough that the origin's response falls within the time horizon of the spacecraft.

6.7. Other motion effects

Closely related to the warping phenomenon is red Doppler shift, which becomes substantial at relativistic speeds (not considered further here). This (as well as relativistic aberration) affects the directivity of transmit and/or receive apertures, detectors, etc. On longer missions multiple receivers are needed to deal with a wide variation in received wavelength, or alternatively the transmitter has to employ multiple compensatory wavelengths to hold the receive wavelength in a narrower range.

Due to both red shift and timebase expansion, the signal power decreases substantially from transmitter to receiver. Power and energy are conspicuously not conserved when they are compared with respect to two distinct frames of reference, the origin and the spacecraft. Reduced signal power substantially reduces the data rate and data volume that can be achieved, and this effect increases as long as the constant self-acceleration continues.

7. Canonical mission trajectory

The kinematic variables in the specific context of the canonical mission scenario (defined in §3.2) are illustrated in Fig.21. Although the trajectory of a spacecraft $C3$ on a canonical mission could be calculated directly from the modeling DEs given by SR, it is easier to recognize the symmetry of canonical self-acceleration. In particular, the trajectory for the second half of the cruise phase is related to the trajectory in the first half (see §6.4) with time running backward, from maximum to zero map-speed (rather than the other way around). The second half of the $C3$ trajectory is thus the mirror image of the first half of the $C1$ trajectory.

To determine that mirror image the two times $\{\tau_h, t_h\}$ at the halfway point ($r_c[t_h] = D/2$) are needed. These are determined from Eq.(14) to be

$$\tau_h = t_H \cdot \cosh^{-1} \left(1 + \frac{D}{2c \cdot t_H} \right) \quad \text{and} \quad t_h = \frac{D}{2c} \sqrt{1 + \frac{4c \cdot t_H}{D}}. \quad (20)$$

It can be verified that $t_h \rightarrow (t_H + D/2c)$ as $D \rightarrow \infty$, or in words t_h at longer distances approaches the coordinate time at which a photon emitted from the origin at $t_o = t_H$ reaches the halfway point.

The second half of the canonical trajectory equals the first half reversed in time, but in addition displaced in both coordinate time (by t_h) as well as in

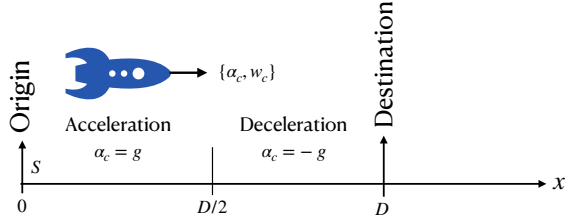


Figure 21: A spacetime coordinate system and the kinematic variables describing the trajectory of a spacecraft relative to an inertial frame S with coordinates defined in Fig.2. Added variables are the self-acceleration α_c and traveler's map-speed w_c , which are both implicitly a function of traveler's time τ_c . For the canonical 1-g launch-landing mission of Fig.1, the acceleration has only two constant values of acceleration, $\alpha_c = \pm g$.

map-position (by $D/2$). Taking these three factors into account, the canonical trajectory becomes

$$\{t_{c3}[\tau_{c3}], r_{c3}[\tau_{c3}]\} = \begin{cases} \{\tau_{c3}, 0\}, & \tau_{c3} < 0 \\ \{t_{c1}[\tau_{c3}], r_{c1}[\tau_{c3}]\}, & 0 \leq \tau_{c3} \leq \tau_h \\ \{2t_h - t_{c1}[2\tau_h - \tau_{c3}], D - r_{c1}[2\tau_h - \tau_{c3}]\}, & \tau_h < \tau_{c3} \leq 2\tau_h \\ \{2t_h + \tau_{c3} - 2\tau_h, D\}, & 2\tau_h < \tau_{c3}. \end{cases} \quad (21)$$

8. Conclusions

The timing relationship (characterized by the clock image functions, in terms of local traveler's clocks) between photon emission and detections as measured at the origin of launch, and one or two accelerating spacecraft, and a landing destination has been characterized by drawing on SR. The methods employed apply generally to accelerated bodies performing photon transfer in their communications. Here they have been applied in two simple cases of one or two spacecraft experiencing indefinite fixed self-acceleration and a canonical launch-landing mission. From these results, the query-response latencies are inferred directly through the composition of two appropriate clock image functions.

The overall conclusion is that these round-trip latencies in both directions are a significant issue for interstellar travel, and in fact such two-way communication is for all practical purposes very cumbersome (due to large latencies) except in the vicinity of the origin or the destination. Interstellar spacecraft and their

crews must accept highly autonomous operations, and abandon notions of maintaining operational and social interactions with those at the origin or destination throughout the mission, with the exception of a short period following launch or prior to landing. Since the root cause is the large propagation distances, this general conclusion applies to many other types of interstellar missions largely irrespective of spacecraft speeds.

There are other issues in inter-traveler communications arising out of relativistic effects that have not been considered here. These include aperture and antennae beam patterns as affected by a significant red shift in wavelength as well as relativistic aberration. Gravitational effects, which have also been neglected, are a factor in the vicinity of origin and destination.

Acknowledgements

The research represented in this tutorial review was supported by a grant from the Breakthrough Foundation and its Breakthrough StarShot program, NASA grants NIAC Phase I DEEP-IN – 2015 NNX15AL91G and NASA NIAC Phase II DEIS – 2016 NNX16AL32G and the NASA California Space Grant NASA NNX10AT93H, the Emmett and Gladys W. Technology Fund, and the Limitless Space Institute.

Appendix A. Nomenclature

S	A one-dimensional (rectilinear) inertial frame with map-position (spatial) and coordinate time $\{x, t\}$
c	Speed of light in a vacuum as observed by any two synchronized coordinate-time clocks in an arbitrary inertial frame S
$\{\mathcal{A}, \mathcal{B}\}$	Accelerated travelers observing traveler's times $\{\tau_a, \tau_b\}$ (in a degenerate case, may also be at rest)
\mathcal{O}	Location of the origin of a spacecraft launch, assumed to be at rest in S
C	A spacecraft, in motion and accelerating during its cruise phase
\mathcal{D}	Location of the destination for a spacecraft, assumed to be at rest in S
D	The fixed distance from \mathcal{O} to \mathcal{D}
MET	Mission elapsed time (initialized at the instant of launch)
τ_a	Traveler's time measured by a clock carried by traveler \mathcal{A}

METT	The MET as measured by the spacecraft traveler's clock
$t_a[\tau_a]$	Coordinate time measured by a (typically notional) clock \mathcal{A} at rest in an inertial frame S at the instantaneous map-position of \mathcal{A} at its traveler's time τ_a
MECT	The MET as measured by a (typically notional) coordinate clock at rest at the instantaneous map-position of the spacecraft
$\pm\alpha$	A spacecraft traveler's self-acceleration ($0 < \alpha$); if positive, this is an acceleration, and if negative, this is a deceleration
t_H	The time horizon of an accelerating spacecraft, equal to α/c
g	Acceleration equal to that experienced at the Earth's surface due to gravity
$\Psi_{\mathcal{A}\Rightarrow\mathcal{B}}[\tau_a]$	Clock image (\mathcal{B} 's traveler's arrival time) in photon exchange for a photon propagating in the direction $\mathcal{A}\Rightarrow\mathcal{B}$ that was emitted by \mathcal{A} at its traveler's time τ_a
$\Omega_{\mathcal{A}\Rightarrow\mathcal{B}}[\tau_b]$	Inverse clock image (\mathcal{A} 's traveler's photon emission time) in photon exchange for a photon propagating in the direction $\mathcal{A}\Rightarrow\mathcal{B}$ that arrives at \mathcal{B} 's traveler's time τ_b
$\mathcal{L}_{\mathcal{A}\Rightarrow\mathcal{B}}[\tau_a]$	Query-response latency (elapsed traveler's time) for queries originating with \mathcal{A} traveler's time τ_a , directed at \mathcal{B} with an immediate response back to \mathcal{A}
$x_a[t_a[\tau_a]]$	Map-position of \mathcal{A} at coordinate time $t_a[\tau_a]$ corresponding to traveler's time τ_a
$r_a[\tau_a]$	Map-position of \mathcal{A} at traveler's time τ_a , equal to $x_a[t_a[\tau_a]]$
$\gamma_a[\tau_a]$	Time-speed (Lorentz factor) for \mathcal{A} at traveler's time τ_a , equal to the derivative of $t_a[\tau_a]$ with respect to τ_a
$w_a[\tau_a]$	Map-speed of \mathcal{A} as measured using map-position $r_a[\tau_a]$ in conjunction with traveler's clock τ_a
$u_a[t[\tau]]$	Map-speed of \mathcal{A} as measured using map-position $x_a[t_a[\tau_a]]$ in conjunction with coordinate clock $t_a[\tau_a]$, both measured at traveler's time τ_a
$w'_a[\tau_a]$	Map-acceleration as measured using map-speed $w_a[\tau_a]$ in conjunction with traveler's clock τ_a
{C1,C2}	Two spacecraft launched at different times, with C1 launched prior to C2

ϵ For a second spacecraft $C2$, the delay in its launch relative to a first spacecraft $C1$, expressed as a fraction of the time horizon t_H (so $0 < \epsilon < 1$)

Appendix B. Analytical results for indefinite acceleration

The assumption of indefinite fixed-magnitude self-acceleration yields straightforward analytical results, which are now derived.

Appendix B.1. Spacecraft trajectory

The trajectory of the spacecraft of Eq.(14) is now derived. Solving differential equation Eq.(13) with initial condition $w_c[0]=0$ and substituting the resulting $w_c[\tau_c]$ into Eq.(12) yields

$$w_c[\tau_c] = c \cdot \sinh(\tau_c/t_H) \quad (\text{B.1a})$$

$$\gamma_c[\tau_c] = \cosh(\tau_c/t_H), \quad (\text{B.1b})$$

Note that c as a subscript in Eq.(B.3) is distinct from c as a physical constant (the speed of light). Solving the differential equation $t'[\tau_c] = \gamma_c[\tau_c]$, substituting Eq.(B.1b) and with initial condition $\tau_c[0]=0$, yields Eq.(14a).

The map-position can be recast as

$$r'_c[\tau_c] = x'_c[\tau_c[\tau_c]] \cdot \gamma_c[\tau_c] = u_c[\tau_c[\tau_c]] \cdot \gamma_c[\tau_c] = w_c[\tau_c], \quad (\text{B.2})$$

from Eq.(11). The $r_c[\tau_c]$ in Eq.(14b) is the solution to differential equation Eq.(B.2) after substituting from Eq.(B.1a) with initial condition $r_c[0]=0$. The canonical mission trajectory is readily inferred from this simpler mission (see §7).

Appendix B.2. Clock images and query-response latency

Consider the trajectory of a photon emitted from position $\{0, t_0\}$ in direction $O \Rightarrow C$ and intersecting the spacecraft trajectory at $\{r_c[\tau_c], t_c[\tau_c]\}$, and also a photon emitted in direction $C \Rightarrow O$ from the spacecraft position $\{r_c[\tau_c], t_c[\tau_c]\}$ that intersects origin $\{0, t_0\}$. Then the respective photon trajectories, based on range equation Eq.(15), are

$$O \Rightarrow C: t_c[\tau_c] = t_o + r_c[\tau_c]/c \quad (\text{B.3a})$$

$$C \Rightarrow O: t_o = t_c[\tau_c] + r_c[\tau_c]/c. \quad (\text{B.3b})$$

The clock images can be determined numerically by calculating t_o for a set of different values of τ_c in Eq.(B.3) (and equivalent relations for the destination).

This yields a list of $\{\tau_o, \tau_c, \tau_d\}$ triplets which directly sample the relevant clock images. This approach was used to generate Fig.8, Fig.9, Fig.13 and Fig.14.

For simple trajectory Eq.(14), analytical results are easily obtained, and these provide additional insight. The clock images in Eq.(17) are the solutions (with the trajectory variables substituted from Eq.(14)) to Eq.(B.3a) for τ_c and to Eq.(B.3b) for $t_o \equiv \tau_o$. Similarly, the inverse clock images in Eq.(18a) and Eq.(18b) are the solutions to Eq.(B.3a) for $t_o \equiv \tau_o$ and to Eq.(B.3b) for τ_c . The query-response latencies associated with the indefinite self-acceleration trajectory of Eq.(19) follow directly from Eq.(17) substituted into Eq.(7).

Appendix B.3. Communication between two accelerating spacecraft

Consider two spacecraft, each with indefinite acceleration as shown in Fig.15, which permits communication between the spacecraft in both directions under some conditions. Analytical results for clock images are readily obtained as an extension of the range equation technique used in §Appendix B.2.

The two spacecraft are labeled $C1$ (the earliest launch) and $C2$ (the later launch). It is assumed that $C2$ is launched at coordinate time $t_o = \epsilon t_H$, and as well that the traveler's clock for $C2$ is initialized to $\tau_{c2}=0$ at that instant of launch. We must have $0 < \epsilon < 1$, or else all photon emissions from $C2$ violate the event horizon of $C1$ and thus will never be detected. In that case the trajectory of $C2$ is identical to that of $C1$ except that it is shifted up by ϵt_H in the time direction. Analogously to Eq.(B.3), the three points at which the trajectory of a photon emitted from O and travelling in the $+x$ direction intersects the trajectories of $C2$ and $C1$ are then given by

$$t_o = t_{c1}[\tau_{c1}] - r_{c1}[\tau_{c1}]/c = \epsilon t_H + t_{c2}[\tau_{c2}] - r_{c2}[\tau_{c2}]/c. \quad (\text{B.4})$$

Substituting for $\{r_c, t_c\}$ from Eq.(14a) and solving for each traveler's time in terms of the other yields the image function for photon exchanges in the direction $C2 \Rightarrow C1$,

$$\Psi_{C2 \Rightarrow C1}[\tau_{c2}] = -t_H \cdot \log \left(e^{-\tau_{c2}/t_H} - \epsilon \right), \quad 0 \leq \tau_{c2} < -t_H \cdot \log \epsilon \quad (\text{B.5a})$$

$$\Omega_{C2 \Rightarrow C1}[\tau_{c1}] = -t_H \cdot \log \left(e^{-\tau_{c1}/t_H} + \epsilon \right), \quad 0 \leq \tau_{c1}. \quad (\text{B.5b})$$

There is an upper bound on the time over which $C2$ can communicate with $C1$; namely, only as long as $C2$ remains within the time horizon of $C1$.

Likewise, a photon emitted in direction $C1 \Rightarrow C2$ from either $C1$ or $C2$ and reaching O at the same t_o must satisfy the range equations

$$t_o = t_{c1}[\tau_{c1}] + r_{c1}[\tau_{c1}]/c = \epsilon t_H + t_{c2}[\tau_{c2}] + r_{c2}[\tau_{c2}]/c. \quad (\text{B.6})$$

Solving for the clock image functions in this direction,

$$\Psi_{C1 \Rightarrow C2}[\tau_{c1}] = t_H \cdot \log\left(e^{\tau_{c1}/t_H} - \epsilon\right), \quad t_H \cdot \log(1 + \epsilon) \leq \tau_{c1} \quad (\text{B.7a})$$

$$\Omega_{C1 \Rightarrow C2}[\tau_{c2}] = t_H \cdot \log\left(e^{\tau_{c2}/t_H} + \epsilon\right), \quad 0 \leq \tau_{c2}. \quad (\text{B.7b})$$

There is a lower limit on τ_{c1} since earlier emissions would arrive prior to launch.

The query-response latencies follow from substituting Eq.(B.5) and Eq.(B.7) into Eq.(7),

$$\mathfrak{L}_{C2 \Leftrightarrow C1}[\tau_{c2}] = t_H \cdot \log\left(\frac{1}{e^{-\tau_{c2}/t_H} - \epsilon} - \epsilon\right) - \tau_{c2}, \quad 0 \leq \tau_{c2} < -t_H \cdot \log \epsilon \quad (\text{B.8a})$$

$$\mathfrak{L}_{C1 \Leftrightarrow C2}[\tau_{c1}] = -t_H \cdot \log\left(\frac{1}{e^{\tau_{c1}/t_H} - \epsilon} - \epsilon\right) - \tau_{c1}, \quad (\text{B.8b})$$

$$t_H \cdot \log(1 + \epsilon) \leq \tau_{c1} < t_H \cdot \log\left(\epsilon + \frac{1}{\epsilon}\right).$$

The upper bound on τ_{c1} in $\mathfrak{L}_{C1 \Leftrightarrow C2}$ follows because the arrival time of a query at C2 must fall within the allowed emission time given in Eq.(B.5a). The upper bound as referred to τ_{c1} is found by applying the inverse clock image in Eq.(B.7b),

$$\Omega_{C1 \Rightarrow C2}(-t_H \cdot \log \epsilon) = t_H \cdot \log\left(\epsilon + \frac{1}{\epsilon}\right). \quad (\text{B.9})$$

The resulting $\mathfrak{L}_{C2 \Leftrightarrow C1}$ and $\mathfrak{L}_{C1 \Leftrightarrow C2}$ are plotted in Fig.18 and Fig.19.

Appendix B.4. Time warping derivatives

The derivatives in Eq.(8) can be derived analytically by taking the total derivative of the range equations [1]. Alternatively they can be expressed in terms of clock images as

$$\left. \frac{d\tau_c}{d\tau_o} \right|_{O \Rightarrow C} = \left(\frac{d}{d\tau_o} \Psi_{O \Rightarrow C}[\tau_o] \right)_{\tau_o = \Omega_{O \Rightarrow C}[\tau_c]} \quad (\text{B.10a})$$

$$\left. \frac{d\tau_o}{d\tau_c} \right|_{C \Rightarrow O} = \frac{d}{d\tau_c} \Psi_{C \Rightarrow O}[\tau_c]. \quad (\text{B.10b})$$

Both derivatives are evaluated at the same spacecraft traveler's time τ_c . Substituting from Eq.(17) and Eq.(18), both derivatives evaluate to the same value, that given in Eq.(8). In addition, the ratio of clock images in Eq.(8) evaluates to that same value when substituted from Eq.(17b) and Eq.(18a).

References

- [1] D. G. Messerschmitt, Relativistic timekeeping, motion, and gravity in distributed systems, *Proc. IEEE* 105 (8) (2017) 1511.
- [2] M. P. Hobson, G. P. Efstathiou, A. N. Lasenby, *General relativity: An introduction for physicists*, Cambridge University Press, 2006.
- [3] W. Bade, Relativistic rocket theory, *American Journal of Physics* 21 (4) (1953) 310–312.
- [4] R. Forward, A transparent derivation of the relativistic rocket equation, in: *31st Joint Propulsion Conference and Exhibit*, 1995, p. 3060.
- [5] A. P. French, *Special relativity*, CRC Press, 1968.
- [6] R. Resnick, *Introduction to special relativity*, Wiley, 2007.
- [7] W. Rindler, *Introduction to special relativity*, Clarendon Press, 1991.
- [8] P. Fraundorf, A one-map two-clock approach to teaching relativity in introductory physics, *arXiv preprint physics/9611011* (1996).
- [9] P. Fraundorf, Some minimally-variant map-based laws of motion at any speed (1997).
- [10] P. Fraundorf, One-map two-clock relativity for introductory physics classes, in: *APS April Meeting Abstracts*, Vol. 1, 1997, p. 1110.
- [11] U. Walter, Relativistic rocket and space flight, *Acta Astronautica* 59 (6) (2006) 453–461.
- [12] S. Westmoreland, A note on relativistic rocketry, *Acta Astronautica* 67 (9-10) (2010) 1248–1251.